



Dipankar Mitra, Mojtaba Afshar

## ABSTRACT

A stepper motor system is essentially an open-loop position control system. There is no feedback to let the driver IC know if the motor is running or stalled. However, in many applications, the user needs to know the status of the motor – either for diagnostics purpose or for position sensing. Sensorless stall detection solutions available in the market today do not detect stalls reliably across wide range of operating parameters such as supply voltage, temperature, and micro-stepping modes. Texas Instruments devices including [DRV8889-Q1](#), [DRV8434A-Q1](#), [DRV8434A](#), [DRV8434S](#), [DRV8452](#), [DRV8461](#), and [DRV8462](#) implement a novel approach of sensorless stall detection of stepper motors by using the PWM off-time to sense the back-EMF. This stall detection algorithm eliminates first-order dependency on supply voltage, coil resistance, and temperature changes. The goal of this application report is to highlight the advantages of the stall detection algorithm of the Texas Instruments devices with stall detection and provide examples of how they can detect stall reliably in a wide variety of end applications.

## Table of Contents

<b>1 Introduction</b> .....	3
<b>2 Back EMF for a Stepper Motor</b> .....	4
<b>3 Existing Stall Detection Schemes</b> .....	5
3.1 Measuring Back EMF During Current Zero Cross.....	5
3.2 Fixed OFF-time Method.....	5
3.3 PWM Cycle-Counting Method.....	6
<b>4 TI Integrated Stall Detection Algorithm</b> .....	7
4.1 Details of the Stall Detection Scheme.....	7
4.2 Details of the Stall Detection structure.....	9
4.3 Details of the Stall Detection Configuration.....	12
4.4 Experimental Results for Stall Detetion Feature.....	15
<b>5 Evaluation Examples</b> .....	31
5.1 Automotive Headlight Leveling and Swivel.....	31
5.2 Automotive Head-up Display (HUD).....	35
5.3 HVAC Valve Control.....	35
<b>6 Summary</b> .....	36
<b>7 References</b> .....	36
<b>8 Revision History</b> .....	38

## List of Figures

Figure 2-1. Back-EMF Phase Shift With Coil Current.....	4
Figure 3-1. Fixed OFF-time Method.....	5
Figure 4-1. Fixed Ripple Current Control Method.....	7
Figure 4-2. Back EMF for Unloaded Motor.....	8
Figure 4-3. PL35L-024 Stepper Motor used in Automotive Application.....	15
Figure 4-4. Coil Current and Torque Count When Motor is Running.....	16
Figure 4-5. Coil Current and Torque Count When Motor is Stalled.....	16
Figure 4-6. Torque Count of the PL35L-024 Motor for DRV8889.....	17
Figure 4-7. Torque Count of the PL35L-024 Motor for DRV8434S with Disabled Torque Scale.....	17
Figure 4-8. Torque Count of the PL35L-024 Motor for DRV8434S with Enabled Torque Scale.....	18
Figure 4-9. Steady Count Variation with Speed for Different Directions of Motion.....	19
Figure 4-10. Stall Count Variation With Direction of Motion.....	19
Figure 4-11. Steady Count at 150 pps for DRV8889-Q1.....	20
Figure 4-12. Steady Count at 150 pps for DRV8434S with Disabled TRQ_SCALE.....	20

Figure 4-13. Steady Count at 150 PPS for DRV8434S with Enabled TRQ_SCALE.....	21
Figure 4-14. Steady Count at 100 PPS for DRV8889-Q1.....	21
Figure 4-15. Steady Count at 100 PPS for DRV8434S with Disabled TRQ_SCALE.....	22
Figure 4-16. Steady Count at 100 PPS for DRV8434S with Enabled TRQ_SCALE.....	22
Figure 4-17. Steady Count at 200 PPS.....	23
Figure 4-18. Steady Count at 700 PPS.....	24
Figure 4-19. Steady Count Change When Q1 Regulation is Lost.....	25
Figure 4-20. Steady Count at 1100 PPS.....	26
Figure 4-21. Steady Count Variation With Supply Voltage.....	27
Figure 4-22. Steady Count Variation With Microstepping.....	27
Figure 4-23. Steady Count Variation With Output Slew Rate.....	28
Figure 4-24. Steady Count Variation With Ambient Temperature.....	28
Figure 4-25. Steady Count Variation With Full-scale Current.....	29
Figure 4-26. Coil Current Waveform for a Valve Motor With 80-Ω Resistance.....	30
Figure 4-27. Coil Current Waveform for a Valve Motor With 36-Ω Resistance.....	30
Figure 4-28. Steady-State Torque Count Variation.....	31
Figure 5-1. Steady Count Across Operating Conditions.....	32
Figure 5-2. Stall Detection of a Headlight Module With DRV8889-Q1.....	33
Figure 5-3. Audio Noise Spectrogram Without Stall Detection.....	33
Figure 5-4. Audio Noise Spectrogram With DRV8889-Q1 Stall Detection.....	34
Figure 5-5. Audio Noise SPL Plot With and Without Stall Detection.....	34
Figure 5-6. Stall Detection.....	35
Figure 5-7. HVAC Valve Steady Count.....	36

### List of Tables

Table 4-1. Drivers With Integrated Stall Detection.....	7
Table 4-2. TI Stepper Drivers with Stall Detection Comparison.....	8
Table 4-3. DRV8889-Q1 Register Map.....	9
Table 4-4. DRV8434S Register Map.....	9
Table 4-5. Fault Condition Summary.....	10
Table 4-6. DRV8434A, DRV8434A-Q1 Stall relevant pins.....	11
Table 4-7. STL_MODE and TRQ_CNT/STL_TH pins configuration summary.....	12
Table 4-8. STL_REP pin configuration summary.....	12
Table 5-1. Operating Conditions for Headlight Stepper Motor.....	31
Table 5-2. Operating Conditions for HUD Module.....	35
Table 5-3. Operating Conditions for HVAC Valve.....	36

### Trademarks

All trademarks are the property of their respective owners.

## 1 Introduction

The simplicity of the open-loop stepper motor system is attractive; however, even in a stepper motor, feedback can be desirable. Many applications require the system to know the state of the motor either for diagnostics purposes, such as being able to detect if the motor is jammed or overloaded; and also, for position sensing to be able to detect if the motor has reached the end of line or hit a physical obstruction.

Applications often severely over-drive the motor beyond the desired end point to ensure the end point is reached, reducing the efficiency of the system. External components to monitor rotor position, such as encoders or Hall sensors add cost to the system. Without stall detection, the motor driver will continue to drive through the obstacle, causing audible noise and mechanical failures.

An integrated sensorless stall detection method can address these negative effects and ensure that the motor is not overloaded or obstructed. Moreover, in situations where precise position sensing is not required, sensorless stall detection can replace expensive Hall sensors, limit switches, and encoders. Integrated sensorless stall detection also provides immediate response when a stall occurs compared to the position sensor solution which requires a timeout mechanism.

A few of the systems and applications which can benefit from an integrated sensorless stall detection algorithm are:

- Automotive headlight leveling and swivel
- Automotive Head-Up Display (HUD)
- Automotive and Industrial HVAC actuator control
- Electronic Expansion Valves (EEV)
- Multi-function printers
- 3-D printers
- Surveillance cameras (pan and tilt motion)
- Medical applications

## 2 Back EMF for a Stepper Motor

For a stepper motor, the supply voltage can be expressed with [Equation 1](#).

$$V_M = I \times R_{\text{coil}} + \text{BEMF} + L \times \frac{di}{dt} \quad (1)$$

where

- $I$  is the coil current
- $R_{\text{coil}}$  is the coil resistance of the motor coil
- BEMF is the back-EMF voltage
- $L$  is the inductance of the coil

The back EMF is the voltage generated by the motor as the armature spins inside the stator. The back EMF can be expressed using [Equation 2](#).

$$\text{BEMF} = -p \times \psi_m \times \omega \times \sin(p\omega t) \quad (2)$$

where

- $p$  is the number of pole pairs
- $\psi_m$  is the maximum magnetic flux, constant for each motor
- $\omega$  is the angular speed of the motor

Therefore, the back EMF is sinusoidal in nature and directly proportional to the motor speed ( $\omega$ ). A motor, when spinning fast, will produce more back EMF than when spinning slower. And when the motor is stalled, no back EMF is produced.

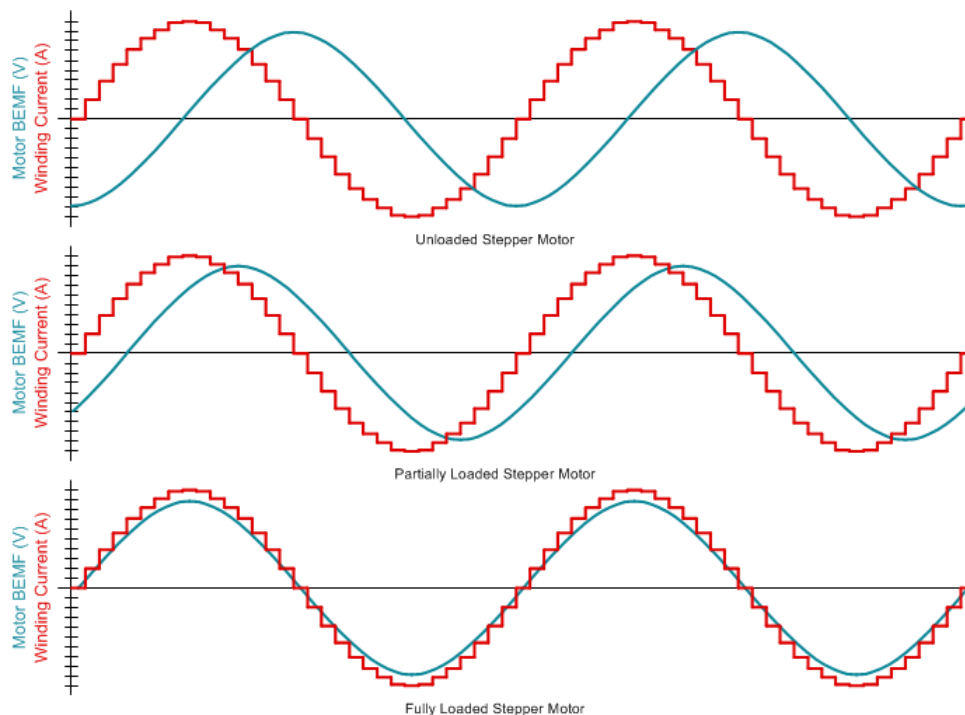


**Figure 2-1. Back-EMF Phase Shift With Coil Current**

Stepper motors have a distinct relation between the coil current, back EMF, and mechanical torque load of the motor, shown in [Figure 2-1](#). Compared to the coil current, the back EMF will be phase-shifted by  $90^\circ$  for an unloaded motor. As the motor load approaches the torque capability of the motor at a given coil current, the back EMF moves in phase with the coil current. When the load torque increases beyond the fully-loaded condition, the rotor falls out of synchronization with the stator magnetic field, causing the motor to stall.

The maximum torque that can be applied to a motor operating at a given speed without losing synchronization is called the pull-out torque. Therefore, a stall condition occurs when the load torque on a motor exceeds the pull-out torque of the motor. Most stepper motor data sheets include pull-out torque vs. speed curves. The pull-out torque will decrease as the speed increases and increase as the current through the motor coils increases.

### 3 Existing Stall Detection Schemes

Multiple sensorless stall detection schemes are available today from various stepper driver manufacturers. A short description of those methods follows:

#### 3.1 Measuring Back EMF During Current Zero Cross

Most stall detection schemes currently available measure back EMF during sinusoidal current zero crossing. When the coil current is zero, the voltage across the motor coil is equal to the back EMF. As the motor stalls, the back EMF drops to a value close to zero. Therefore, when the back EMF decreases, it gives a good indication that the motor has stalled.

However, this method has certain drawbacks, such as:

- Back EMF is only monitored during zero crossing.
- The measurement window needs to ensure that the coil current has really reached zero. Ringing in the coil voltage waveform around the zero crossing point can shorten the measurement window and extra blanking time might be needed.
- For high motor speeds, this method needs complicated circuitry for fast measurement. So, this method does not work above moderately high motor speeds.
- This method does not work in *Full Step* mode - coil current switches between 71% and -71% of full-scale setting; therefore, zero-cross detection is not possible. Some methods force a zero-cross period even in full-step mode - but that approach has its own issues.
- When the motor is spinning slowly, the change in back EMF can be hard to detect.

#### 3.2 Fixed OFF-time Method

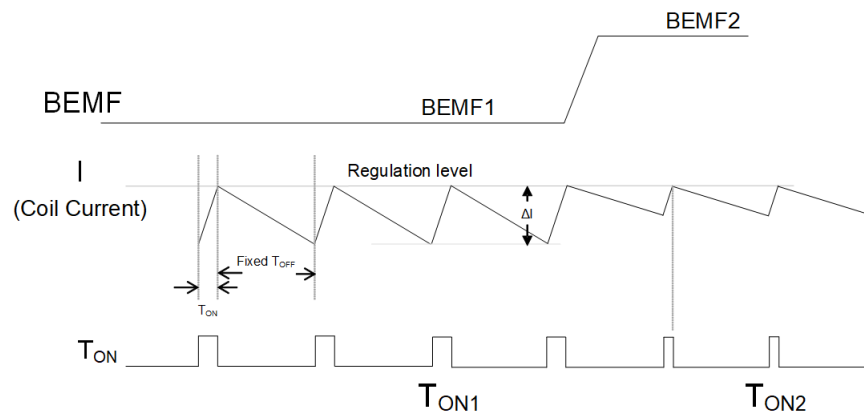


**Figure 3-1. Fixed OFF-time Method**

Some fixed PWM OFF-time ( $T_{OFF}$ ) current regulation methods depend on the difference between PWM on times ( $T_{ON}$ ) in successive cycles to determine back EMF and therefore detect stall, as [Figure 3-1](#) shows.

However, this method has its own drawbacks as well. The equation for the on time is shown by [Equation 3](#):

$$T_{ON} = T_{OFF} \times \frac{((I \times R) - BEMF)}{(VM - ((I \times R) - BEMF))} \quad (3)$$

$$\Delta T_{ON} = T_{ON1} - T_{ON2} = T_{OFF} \times \frac{VM \times (BEMF2 - BEMF1)}{(VM - (I \times R) - BEMF1) \times (VM - (I \times R) - BEMF2)} \quad (4)$$

As is evident from [Equation 4](#),  $\Delta T_{ON}$  depends on supply voltage, coil current and coil resistance (and therefore ambient temperature). So, this scheme can potentially result in false and missed stall detection when supply voltage, temperature, or motor current changes.

### 3.3 PWM Cycle-Counting Method

Some implementations monitor PWM cycle count to sense back EMF changes, and thereby detect stall. Back EMF decreases at stall condition, allowing faster current rise time. At fixed step frequency, stall results in more PWM cycles per step (due to fixed TOFF). Drawbacks of this method are:

1. As can be seen from [Equation 3](#),  $T_{ON}$  is going to vary based on supply voltage (VM), motor current (I), and temperature (T) (motor resistance R increases with T). Therefore, this method might result in false and missed stall detection when the supply voltage, temperature, or motor current changes.
2. Does not work in Full Step mode
3. Works only when the step frequency is relatively constant. If the step frequency changes dynamically, it creates uncertainty in the number of PWM pulses.

## 4 TI Integrated Stall Detection Algorithm

The stepper motor drivers from TI which integrated stall detection feature are listed in [Table 4-1](#).

**Table 4-1. Drivers With Integrated Stall Detection**

Device	Market	Voltage Range	Maximum Current	Interface
<a href="#">DRV8889-Q1</a>	Automotive	4.5 - 45 V	1.5 A	SPI
<a href="#">DRV8434A</a>	Industrial	4.5 - 48 V	2.5 A	GPIO
<a href="#">DRV8434S</a>	Industrial	4.5 - 48 V	2.5 A	SPI
<a href="#">DRV8452</a>	Industrial	4.5 - 55 V	5 A	SPI
<a href="#">DRV8461</a>	Industrial	4.5 - 65 V	3 A	SPI
<a href="#">DRV8462</a>	Industrial	4.5 - 65 V	10 A	SPI

[DRV8889-Q1](#) was the first stepper driver from TI to integrate stall detection feature, meant mostly for automotive applications. A slightly updated scheme has been used in the rest of the drivers to be able to detect stall at relatively higher motor speeds typically seen in industrial applications. The following sections explain the stall detection scheme in detail.

### 4.1 Details of the Stall Detection Scheme

[Figure 2-1](#) shows that for an unloaded motor, back EMF is 90° phase shifted from the motor current. As the load increases, the back-EMF phase shift decreases. Finally, as the load increases to the point where the load torque exceeds the pull-out torque, the motor stalls and the back EMF goes to zero. By detecting back-EMF phase shift between rising and falling current quadrants of the motor current, the Texas Instruments devices with stall detection can detect a motor overload stall condition or an end-of-line travel.

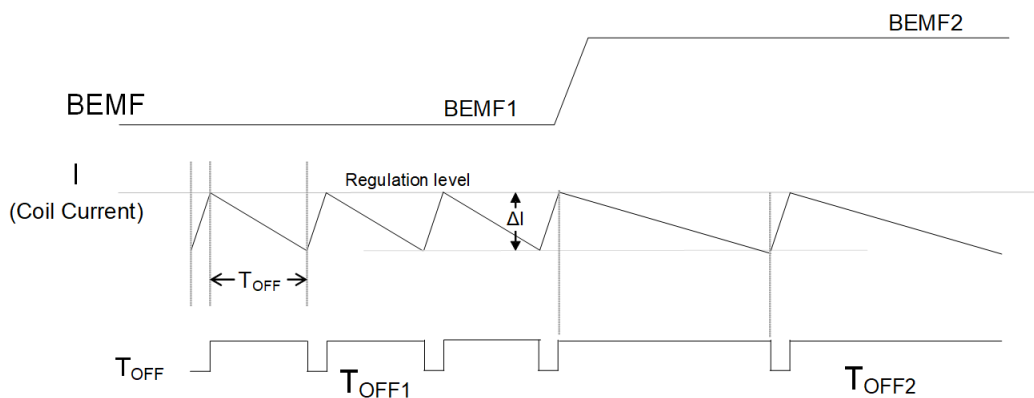


**Figure 4-1. Fixed Ripple Current Control Method**

$$T_{OFF} = \frac{L \times \Delta I}{(I \times R) - BEMF} \quad (5)$$

To overcome the issues associated with fixed  $T_{OFF}$  current regulation method, a fixed ripple current regulation method (smart tune ripple control decay mode) is used by the TI stepper drivers, shown in [Figure 4-1](#). This allows  $T_{OFF}$  to also vary based on back EMF - more back EMF leads to higher  $T_{OFF}$ , and lesser back EMF leads to less  $T_{OFF}$ . By monitoring  $T_{OFF}$ , first order dependency on supply voltage is eliminated, as the VM supply is disconnected from the motor during PWM off time. [Equation 5](#) shows that  $T_{OFF}$  does not depend on VM.

$$\frac{1}{T_{OFF1}} - \frac{1}{T_{OFF2}} = \frac{1}{L \times \Delta I} \times (BEMF2 - BEMF1) \quad (6)$$

Instead of  $T_{OFF}$  delta, the delta of the reciprocal of  $T_{OFF}$  can be used to further eliminate the dependency on  $I$  and  $R$  terms (motor current and resistance/temperature). As Equation 6 shows, delta ( $\frac{1}{T_{OFF}}$ ) does not depend on VM,  $I$ , or  $R$  and only on back EMF change (other terms  $\Delta I$  and  $L$  are current ripple and motor inductance which are constants for a system).

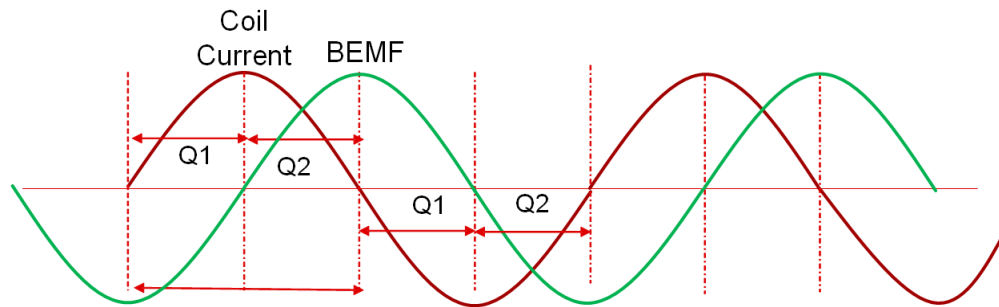


**Figure 4-2. Back EMF for Unloaded Motor**

As Figure 4-2 shows, comparing the back-EMF (by monitoring  $\frac{1}{T_{OFF}}$ ) between the rising (Q1) and falling (Q2) current quadrants of the sinusoidal current can give a good indication of the motor load. For a lightly loaded motor, the delta back EMF between falling and rising quadrant in Figure 4-2 will be a positive value. As the load increases and approaches stall condition, the back-EMF delta between the falling and rising current quadrants will approach zero and can be used to detect the stall condition.

The stall algorithm monitors  $T_{OFF}$  during Q1 and Q2 of each electrical half-cycle. The subtraction between  $\frac{1}{T_{OFF1}}$  (average) and  $\frac{1}{T_{OFF2}}$  (average) happens at the end of each half-cycle. The  $(\frac{1}{T_{OFF1}} - \frac{1}{T_{OFF2}})$  value calculated at the end of a half-cycle is averaged with the values calculated at the end of three previous half-cycles, to arrive at a moving average called torque count TRQ\_COUNT. For a lightly loaded motor, the TRQ\_COUNT settles at a non-zero steady-state value, known as the steady count. As the motor approaches a stall condition, the TRQ\_COUNT gradually decreases, approaching zero, and can be utilized to detect the stall condition. The device detects a stall whenever the TRQ\_COUNT falls below a predefined threshold, referred to as STL\_TH.

#### 4.1.1 TRQ\_COUNT & STL\_TH Bit Resolution

The DRV8889-Q1 device features 8-bit registers for TRQ\_COUNT and STL\_TH, whereas the DRV8434S, DRV8452, DRV8461, and DRV8462 devices offer higher resolution TRQ\_COUNT and STL\_TH values with 12-bit precision. Furthermore, the DRV8434A-Q1, DRV8434A, are hardware devices that provide 12-bit resolution for the TRQ\_CNT/STL\_TH output/input pin, enhancing the accuracy of stall detection. The increase in bit resolution allows for more precision and accuracy in detecting stall conditions. This higher resolution leads to finer distinction between mechanical load changes, meaning more accurate stall detection without false positives or missed stall conditions.

#### 4.1.2 Amplifying Torque Count & Stall Threshold

In applications with high motor coil resistance or low operating speeds, the TRQ\_CNT value is typically low due to reduced BEMF, making stall detection more challenging and unreliable in the DRV8889-Q1. To mitigate this issue, certain devices - including the DRV8434A-Q1, DRV8434A, DRV8434S, DRV8452, DRV8461, and DRV8462 feature a scale-up capability that amplifies the torque count and stall threshold by a factor of 8. By amplifying the torque count, these devices enable more accurate detection even at low BEMF levels, resulting in higher TRQ\_CNT values. The table below compares the TI devices with a stall detection feature.

**Table 4-2. TI Stepper Drivers with Stall Detection Comparison**

Stall Detection Feature	DRV8889-Q1	DRV8434S, DRV8452, DRV8461, DRV8462	DRV8434A-Q1, DRV8434A
Interface	SPI	SPI	Hardware
Torque Count Resolution	8-bit	12-bit	12-bit



**Table 4-2. TI Stepper Drivers with Stall Detection Comparison (continued)**

Stall Detection Feature	DRV8889-Q1	DRV8434S, DRV8452, DRV8461, DRV8462	DRV8434A-Q1, DRV8434A
Stall Threshold Resolution	8-bit	12-bit	12-bit
CTRQ_COUNT / STALL_TH Scale UP	N/A	scaled up by 8	scaled up by 8

## 4.2 Details of the Stall Detection structure

This section discusses about the stall detection configuration in TI stepper drivers with different interface configurations.

### 4.2.1 SPI Interfaces Devices

The [DRV8889-Q1](#), [DRV8434S](#), [DRV8452](#), [DRV8461](#), and [DRV8462](#) provide stall detection capabilities through an SPI interface. The stall parameter settings for these devices can be broadly categorized into two groups. The [DRV8434S](#) shares the same parameters as the [DRV8452](#), [DRV8461](#), and [DRV8462](#), while the [DRV8889-Q1](#) has distinct settings. To provide comprehensive coverage, this section will focus on the [DRV8889-Q1](#) and [DRV8434S](#), representing both categories.

For a detailed understanding of the hardware implementation of the Evaluation Module (EVM) for these devices, please refer to the respective user's guides: the [DRV8889-Q1 Evaluation Module User's Guide](#) and the [DRV8434S-Q1 Evaluation Module User's Guide](#). Additionally, the [DRV8889-Q1 EVM GUI User's Guide](#) and the [DRV8434S EVM GUI User's Guide](#) offer step-by-step instructions on utilizing the graphical user interface (GUI) software with the EVM.

The registers map for the [DRV8889-Q1](#) and [DRV8434S](#) devices are outlined in [Table 4-3](#) and [Table 4-3](#), respectively, providing a detailed overview of the register configurations for each device. It can be seen from the register maps below that [DRV8434S](#) (and similar devices) have two additional registers to support the increase in bit resolution and scalability for STALL\_TH and TRQ\_COUNT.

**Table 4-3. DRV8889-Q1 Register Map**

Register Name	7	6	5	4	3	2	1	0	Access Type	Address
FAULT Status	<b>FAULT</b>	SPI_ERROR	UVLO	CPUV	OCV	<b>STL</b>	TF	OL	R	0x00
DIAG Status 1	OCP_LS2_B	OCP_HS2_B	OCP_LS1_B	OCP_HS1_B	OCP_LS2_A	OCP_HS2_A	OCP_LS1_A	OCP_HS1_A	R	0x01
DIAG Status 2	UTW	OTW	OTS	<b>STL_LRN_OK</b>	<b>STALL</b>	RSVD	OL_B	OL_A	R	0x02
CTRL1	TRQ_DAC [3:0]				RSVD		SLEW_RATE [1:0]		RW	0x03
CTRL2	DIS_OUT	RSVD		TOFF [1:0]		<b>DECAY [2:0]</b>			RW	0x04
CTRL3	DIR	STEP	SPI_DIR	SPI_STEP	MICROSTEP_MODE [3:0]				RW	0x05
CTRL4	CLR_FLT	LOCK [2:0]			EN_OL	OCP_MODE	OTSD_MOD_E	TW_REP	RW	0x06
CTRL5	RSVD		<b>STL_LRN</b>	<b>EN_STL</b>	<b>STL_REP</b>	RSVD			RW	0x07
CTRL6	<b>STALL_TH [7:0]</b>								RW	0x08
CTRL7	<b>TRQ_COUNT [7:0]</b>								R	0x09

**Table 4-4. DRV8434S Register Map**

Register Name	7	6	5	4	3	2	1	0	Access Type	Address
FAULT Status	<b>FAULT</b>	SPI_ERROR	UVLO	CPUV	OCV	<b>STL</b>	TF	OL	R	0x00
DIAG Status 1	OCP_LS2_B	OCP_HS2_B	OCP_LS1_B	OCP_HS1_B	OCP_LS2_A	OCP_HS2_A	OCP_LS1_A	OCP_HS1_A	R	0x01
DIAG Status 2	UTW	OTW	OTS	<b>STL_LRN_OK</b>	<b>STALL</b>	RSVD	OL_B	OL_A	R	0x02
CTRL1	TRQ_DAC [3:0]				RSVD		SLEW_RATE [1:0]		RW	0x03
CTRL2	DIS_OUT	RSVD		TOFF [1:0]		<b>DECAY [2:0]</b>			RW	0x04

**Table 4-4. DRV8434S Register Map (continued)**

Register Name	7	6	5	4	3	2	1	0	Access Type	Address	
CTRL3	DIR	STEP	SPI_DIR	SPI_STEP	MICROSTEP_MODE [3:0]				RW	0x05	
CTRL4	CLR_FLT	LOCK [2:0]			EN_OL	OCP_MODE	OTSD_MODE	TW_REP	RW	0x06	
CTRL5	RSVD		STL_LRN	EN_STL	STL_REP	RSVD			RW	0x07	
CTRL6	STALL_TH [7:0]								RW	0x08	
CTRL7	RC_RIPPLE[1:0]		EN_SSC	TRQ_SCALE	SATLL_TH [11:8]						
CTRL8	TRQ_COUNT [7:0]								R	0x09	
CTRL9	REV_ID [3:0]				TRQ_COUNT [11:8]						

It is fairly straightforward to set up the device for stall detection with only a few bits controlling the critical parameters related to the stall detection algorithm. The bits relevant for stall detection are highlighted in [Table 4-3](#) and [Table 4-3](#).

- **EN\_STL**: By default, stall detection is disabled after the device powers-up. EN\_STL must be set to 01b to enable stall detection.
- **DECAY [2:0]**: The decay mode must be set to smart tune ripple control, therefore it must be ensured that it is set to 111b. Setting the decay mode to any other value will disable stall detection.
- **STL\_LRN**: It is 00b by default. It must be set to 01b to enable the automatic stall learning process. This bit automatically returns to 00b when the stall learning process is complete.
- **STL\_LRN\_OK**: Becomes 01b at the end of successful stall threshold learning.
- **TRQ\_COUNT [7:0]**: These 8 bits reserve the value of TRQ\_CNT, providing an indication of the load torque. The value is inversely proportional to the motor load, being highest when the motor is unloaded and approaching zero as the motor stalls. This allows for assessment of the motor's load status. Furthermore, drivers with 12-bit resolution offer an extended range, with additional TRQ\_COUNT [11:8] bits available in another register, enabling more precise torque monitoring.
- **STALL\_TH [7:0]**: These 8 bits are used to manually program or learn the desired stall threshold level through the stall learning process. Whenever the torque count drops below this threshold, the device detects a stall. Additionally, in devices equipped with a 12-bit stall threshold, a further 4 bits (STALL\_TH [11:8]) are available in another register, providing extended configuration options.
- **STL\_REP**: This bit controls the reporting of stall detection. To enable stall detection fault reporting on the nFAULT pin, the STL\_REP bit must be set to 01b. When this condition is met, the nFAULT pin will be driven low upon detection of a stall, providing a clear indication of the fault.
- **TRQ\_SCALE**: In devices featuring a scale-up capability, this bit can be configured to '1' to enable the scaling up of low TRQ\_COUNT and STALL\_TH values by a factor of 8. Specifically, if the initial TRQ\_COUNT value calculated by the algorithm is less than 500 it is recommended to set the TRQ\_SCALE bit to 01b for detection accuracy improvement.

When a stall is detected, the STALL, STL, and FAULT bits are latched high, and the nFAULT pin is pulled low (if STL\_REP is set to 01b). In this stalled state, the motor shaft comes to a halt, although the motor may still exhibit vibrations if it continues to receive STEP signals. The motor will resume spinning once the stall condition is resolved. The nFAULT signal is released and the fault registers are cleared when a clear faults command is issued, either by setting the CLR\_FLT bit or by applying an nSLEEP reset pulse. For a comprehensive summary of the fault conditions related to stall detection in SPI devices, refer to [Table 4-5](#).

**Table 4-5. Fault Condition Summary**

FAULT	CONDITION	CONFIGURATION	H-BRIDGE	CHARGE PUMP	INDEXER	LOGIC	RECOVERY
Stall Detection (STALL)	Stall / stuck motor	STL_REP = 00b	Operating	Operating	Operating	Operating	CLR_FLT/ nSLEEP
		STL_REP = 01b	Operating	Operating	Operating	Operating	

### 4.2.2 Hardware Interface Devices

The [DRV8434A-Q1](#) and [DRV8434A](#) devices feature hardware stall detection capabilities. For a detailed overview of the hardware implementation, refer to the [DRV8434A Evaluation Module User's Guide](#), which provides a comprehensive description of the EVM. The following table summarizes the key pins relevant to stall detection in the devices with hardware interface, highlighting the key pins and signals involved in stall detection feat.

**Table 4-6. DRV8434A, DRV8434A-Q1 Stall relevant pins**

Pin	Type	Description				
STL_MODE	Input	Pin input level programs the stall detection mode: GND = Torque Count Mode, torque count analog voltage is output on TRQ_CNT/STL_TH pin. Hi-Z = Learning Mode, learning result analog voltage is output on TRQ_CNT/STL_TH pin. DVDD = Stall Threshold Mode, stall threshold is set by an input voltage on the TRQ_CNT/STL_TH pin. Tied to GND with a 330k $\Omega$ resistor = Stall detection disabled.				
TRQ_CNT /STL_TH	Input/output	Torque count analog output or stall threshold analog input depending on the STL_MODE pin input level. A 1nF capacitor must be connected from this pin to GND. STL_MODE = GND, Indicate torque count voltage as output. STL_MODE = DVDD, Program stall threshold voltage as input. STL_MODE = Hi-Z, indicate stall threshold voltage as output.				
STL_REP	Open Drain	Stall fault report output. Requires a pullup resistor ( suggested 10k $\Omega$ ). If this pin is connected to GND, stall fault reporting is disabled. <table border="1" data-bbox="1058 1243 1476 1486"> <tr> <td>STL_MODE = GND/ DVDD</td> <td>A low to high transition on STL_REP pin indicates a stall</td> </tr> <tr> <td>STL_MODE = Hi-Z</td> <td>A high to low transition on STL_REP pin indicates successful learning.</td> </tr> </table>	STL_MODE = GND/ DVDD	A low to high transition on STL_REP pin indicates a stall	STL_MODE = Hi-Z	A high to low transition on STL_REP pin indicates successful learning.
STL_MODE = GND/ DVDD	A low to high transition on STL_REP pin indicates a stall					
STL_MODE = Hi-Z	A high to low transition on STL_REP pin indicates successful learning.					
Enable	Input	0 = Disable device output 1 = Enable device output Hi-Z = Enable device output and 8x torque count scaling				
nFAULT	Output	If STL_REP > 1.6V, nFAULT goes low when stall is detected				

The stall detection algorithm of the [DRV8434A](#) and [DRV8434A-Q1](#) devices is comprehensively configured through a combination of three key pins: two digital IO pins, STL\_MODE and STL\_REP, and one analog IO pin, TRQ\_CNT/STL\_TH. These pins are used to enable precise control and customization of the stall detection functionality. Detailed explanations of the roles, configurations, and applications of these pins are provided

below, offering a thorough understanding of how to optimize the performance of the [DRV8434A](#) and [DRV8434A-Q1](#) in various operating conditions.

#### 4.2.2.1 STL\_MODE and TRQ\_CNT/STL\_TH Pins

The STL\_MODE pin offers versatility through its four configurable states: Low, Hi-z, High, and a connection to ground via a 330kΩ resistor. The specific state of the pin determines the functionality of the stall detection condition and TRQ\_CNT/STL\_TH pin status. These functionalities are outlined in detail in the table below, providing a clear guide to the capabilities and uses of the STL\_MODE pin in different scenarios.

**Table 4-7. STL\_MODE and TRQ\_CNT/STL\_TH pins configuration summary**

Operating Mode	STL_MODE	TRQ_CNT/STL_TH status
Torque Count Mode	GND	Output: Indicate Torque count voltage
Stall Threshold Mode	DVDD	Input: Program stall threshold voltage
Learning Mode	Hi-Z	Output: Indicate stall threshold voltage
Stall Detection Disabled	Tie to GND through 330kΩ	N/A

#### 4.2.2.2 STL\_REP pin

The STL\_REP pin is designated for stall fault reporting, with its functionality disabled when directly connected to ground. To ensure proper operation, an external pull-up resistor is mandatory. A detailed summary of the pin's operational conditions is provided in the table below.

**Table 4-8. STL\_REP pin configuration summary**

Operating Mode	STL_MODE	Condition	STL_REP	nFAULT
Torque Count Mode or Stall Threshold Mode	GND or DVDD	No Stall Report	Pulled Low externally	High
		No Stall Fault	Low	High
		STALL Fault	High	Low (If STL_REP > 1.6V)
Learning Mode	Hi-Z	Learning Successful	Low	N/A
		Learning not done	High	
Stall Detection Disabled	Tie to GND through 330kΩ		Low	

### 4.3 Details of the Stall Detection Configuration

The stall detection algorithm calculates the TRQ\_COUNT value, which serves as a key indicator of motor load conditions. For a lightly loaded motor, TRQ\_COUNT yields a non-zero value, referred to as the steady count. As the motor approaches a stall condition, TRQ\_COUNT decreases towards zero, denoted as the stall count, enabling the detection of stall conditions. A stall is detected when TRQ\_COUNT falls below the predefined threshold. Configuration steps are tailored for SPI-based devices and Hardware-based devices, ensuring optimized performance and detection capabilities.

#### 4.3.1 SPI Interface Devices

To enable stall detection in devices with an SPI interface, such as the [DRV8889-Q1](#), [DRV8434S](#), [DRV8252](#), [DRV8461](#), and [DRV8462](#), follow these steps:

- Enable Stall Detection:** Begin the motor spinning at a normal speed and load current for your application and set EN\_STL to 01b to activate the feature.
- Read Torque Count Value:** Get torque count information by reading the TRQ\_CNT register during normal operation.
- Set Stall Threshold:** Choose from two configuration options:
  - Read TRQ\_CNT register during stall and manually set a specific threshold value by writing to the STALL\_TH bits.
  - Allow the algorithm to automatically learn the ideal threshold value through the stall learning process.

Section [How to Set Stall Threshold in SPI Devices](#) explains steps required for SPI devices to set the stall threshold.

4. **Monitor Stall Reporting:** Receive stall detection reports through various channels, including:
  - a. STALL, STL, and FAULT bits in the DIAG Status 2 and Fault Status registers.
  - b. The nFAULT pin, provided the STL\_REP bit is activated.

For devices equipped with the Torque Scale feature, enable the TRQ\_SCALE bit if the initial TRQ\_COUNT value is less than 500. This allows the TRQ\_COUNT to be multiplied by a factor of 8, effectively scaling the torque measurement to enhance accuracy and precision.

#### 4.3.1.1 How to Set Stall Threshold in SPI Devices

In devices equipped with Stall detection and featuring an SPI interface, the stall threshold can be set in one of two ways: either by manually writing the STALL\_TH bits or by allowing the algorithm to automatically learn the ideal stall threshold value through the stall learning process.

##### 4.3.1.1.1 User-Defined Stall Threshold

Users can write a value to the threshold register if they have torque count information for their use case. They can get torque count information for their use case by reading the TRQ\_CNT register, during normal operation of the motor and when the motor is stalled. The stallthreshold should be set as the average of steady count and stall count. The characterization of the torque count should be done over the entire range of operating conditions (temperature, supply voltage, speed, and so forth) and for both directions of motion. If the operating conditions vary a lot, such as the motor speed changing between high and low values, it may not be possible to set a single stall threshold for all conditions. In this case, the controller may implement a look-up table for the stall threshold. Sometimes, an external low-pass filter with a sufficiently high time-constant might be needed to remove ripples in the torque count due to vibration when the motor is stalled.

##### 4.3.1.1.2 Driver-Defined Stall Threshold

The system itself can go into stall learning mode and calculate the ideal stall threshold for the motor. The following procedure describes the stall learning mode:

- Run motor on no load
- Initiate learning by writing STL\_LRN = 1
- Wait for 32 electrical cycles for the driver to learn the steady count. The time to wait will depend on the step frequency and Microstepping.
- Stall the motor
- Wait for 16 electrical cycles for the driver to learn the stall count
- Read the register until STL\_LRN = 0
- If STL\_LRN\_OK = 1, then the stall threshold value has been calculated. If STL\_LRN\_OK = 0, then the stall learning is not successful.
- Stall threshold is calculated as the average steady count and stall count. At the end of a successful learning, the STALL\_TH register is loaded with the proper stall threshold bits.

In certain scenarios, the stall learning process may not yield accurate results due to fluctuations in the torque count during motor operation or stall. Factors such as high coil resistance or extreme speeds can cause significant variations in the torque count, resulting in a small difference between the steady-state count and the stall count. In such cases, it's recommended to analyze the steady-state count and torque count across the entire operating range and set the threshold at a midpoint between the minimum steady-state count and the maximum stall count

#### 4.3.2 Hardware Interface Devices

To enable stall detection in devices with a Hardware interface, such as [DRV8434A](#) and [DRV8434A-Q1](#), follow these steps.

1. **Enable Stall Detection:** Begin the motor spinning at a normal speed and load current for your application. STL\_MODE programs the stall detection mode. set STL\_MODE pin to GND or DVDD enables the stall detection. STL\_MODE Hi-Z enables learning mode.
2. **Read Torque Count Value:** Connect STL\_MODE pin to GND and measure analog voltage on TRQ\_CNT / STL\_TH pin.

3. **Set the Stall Threshold:** Choose from two configuration options:
  - a. Connect STL\_MODE to DVDD and apply a specific threshold voltage to TRQ\_CNT /STL\_TH pin, this voltage is used as the stall threshold voltage and compare with the internal TRQ\_CNT value.
  - b. Allow the algorithm to automatically learn the ideal threshold value through the stall learning process.

Section [How to set Stall Threshold in Hardware Devcies](#) explains steps required for hardware devices to set the stall threshold.

4. **Monitor Stall Reporting:** The STL\_REP pin is designated for stall fault reporting, with its functionality disabled when directly connected to ground:
  - a. STL\_REP pin at High reports stall fault.
  - b. The nFAULT goes low if STL\_REP > 1.6V.

The TRQ\_SCALE can be enabled by leaving the ENABLE pin float (Hi-Z mode). This allows the TRQ\_COUNT to be multiplied by a factor of 8, effectively scaling the torque measurement to enhance accuracy and precision when the initial TRQ\_COUNT value is less than 500.

#### 4.3.2.1 How to set Stall Threshold in Hardware Devcies

In devices with hardware interface, the stall threshold can be set in one of two ways: user defined stall threshold or driver defined stall thresholds which are explained in detail below.

##### 4.3.2.1.1 User-Defined Stall Threshold

To leverage stall threshold values effectively, users must have access to torque count information specific to their use case. This can be achieved by measuring the torque count voltage on the TRQ\_CNT/STL\_TH pin when the STL\_MODE is connected to GND, under both normal and stall conditions. The average of these measurements can then be used to determine the stall threshold.

There are two methods to detect stall faults based on the determined stall threshold value:

1. **Applying Stall Threshold Voltage to TRQ\_CNT/STL\_TH Pin:** In this mode, users can configure stall detection using the stall threshold information. By connecting the STL\_MODE to DVDD, the device enters stall threshold operating mode. Then, a desired stall threshold voltage is applied to the TRQ\_CNT/STL\_TH pin. This voltage is compared with the internal TRQ\_CNT value. If the internal value falls below the applied threshold, the device reports a stall fault by driving the STL\_REP pin from low to high. Apply nSLEEP reset pulse to pull down STL\_REP and pull up nFAULT again.
2. **MCU-Assisted Stall Detection Mode:** This mode involves the MCU to take the TRQ\_CNT/STL\_TH voltage as input. It compensates for any second-order effects and compares the voltage with its own stall threshold value to detect a stall. To implement this, the STL\_MODE pin should be connected to GND, and the TRQ\_CNT/STL\_TH pin should be connected to the MCU's ADC pin. The MCU then compares the TRQ\_CNT value with its specified stall threshold value and reports a fault if necessary. Since this mode is external, the device's internal stall reporting mechanism must be disabled by connecting STL\_REP pin to GND. Additionally, the MCU can run an algorithm to control VREF based on the torque count, enhancing the detection accuracy and system performance.

##### 4.3.2.1.2 Driver-Defined Stall Threshold

The system features an automatic stall learning mode, which determines the optimal stall threshold for the motor and outputs it as an analog voltage on the TRQ\_CNT/STL\_TH pin. The threshold value is also stored internally for later use in Torque Count Mode to let driver detect the stall fault based on the optimal stall threshold calculated by learning mode. To initiate this process, follow the procedure described below.

1. Before stall threshold learning, ensure that the motor speed has reached its target value. Do not learn stall threshold while the motor speed is ramping up or down.
2. Initiate learning by making the STL\_MODE pin Hi-Z.
3. Run motor with no load.
4. Wait for 32 electrical cycles for the driver to learn the steady count.
5. Stall the motor.
6. Wait for 16 electrical cycles for the driver to learn the stall count.

7. STL\_REP will be pulled low if learning is successful.
8. Stall threshold is calculated as the average of steady count and stall count.
9. At the end of a successful learning, TRQ\_CNT/STL\_TH pin outputs the stall threshold as an analog voltage, and also stores the value internally for use with Torque Count Mode.
10. After successful learning, once device enters Torque Count mode or Stall Threshold mode by changing STL\_MODE logic level, STL\_REP goes high, nFAULT is pulled down and the voltage on the TRQ\_CNT/STL\_TH pin is reset.
11. Apply nSLEEP reset pulse to pull down STL\_REP and pull up nFAULT again

#### 4.4 Experimental Results for Stall Detetion Feature

PL35L-024 stepper motor which is commonly being used in adaptive headlight applications is utilized for stall detection experiments. This motor is rated for maximum 450 mA drive current and the coil has 7.7- $\Omega$  resistance. As shown in [Figure 4-3](#), depending on the direction of motion, the motor shaft moves inside or outside. In devices with 8-bit TRQ\_COUNT (like DRV8889\_Q1), the MSP430 MCU converts the TRQ\_COUNT into an analog voltage, using the 8-bit DAC inside the MCU. The full range of the DAC is 3.3 V, and it corresponds to 256 counts of the TRQ\_COUNT register. Therefore, a single TRQ\_COUNT bit is represented as 12.89 mV. However, in devices with 12-bit TRQ\_COUNT (like DRV8434S), the MSP430 MCU converts the TRQ\_COUNT into an analog voltage, using the 12-bit DAC inside the MCU. The full range of the DAC is 3.3 V, and it corresponds to 4096 counts of the TRQ\_COUNT register. Therefore, a single TRQ\_COUNT value is represented as 0.81 mV.

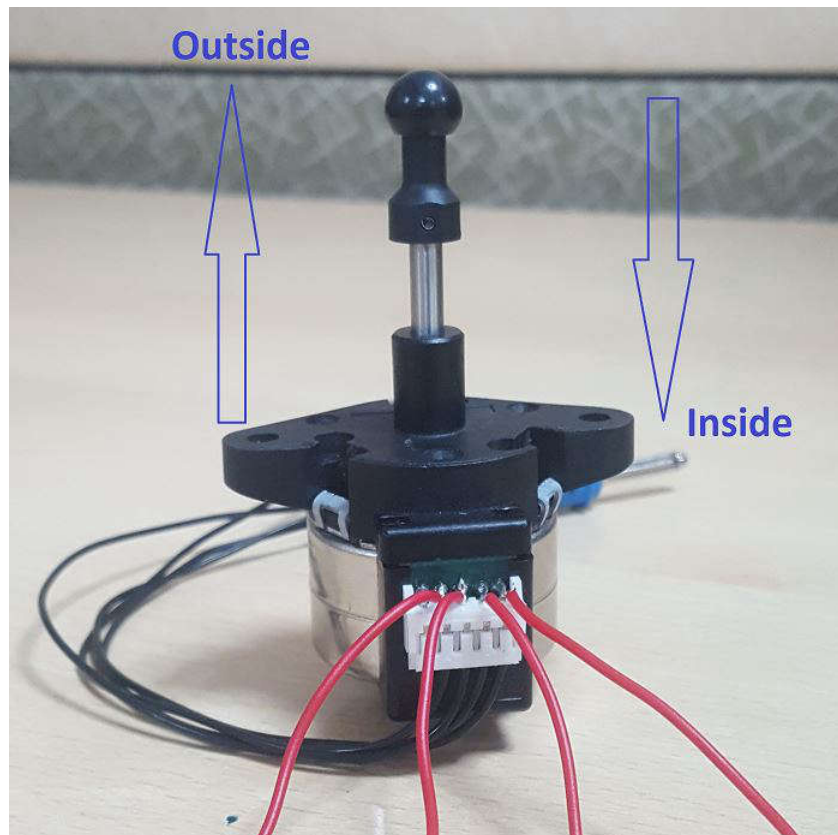


**Figure 4-3. PL35L-024 Stepper Motor used in Automotive Application**

##### 4.4.1 Motor Waveforms Under Normal and Stall condition

[Figure 4-4](#) and [Figure 4-5](#) illustrate the motor coil current, TRQ\_COUNT value, and step pulse under normal and stall conditions, respectively. With a supply voltage of 13.5 V, the DRV8889-Q1 device is configured for full-step mode, operating at a speed of 125 pps, with a full-scale current of 200 mA and a slew rate of 105 V/ $\mu$ s. When the motor reaches either end stop, it becomes stalled. As evident from the figures, when the motor runs

at its nominal speed, the back EMF distorts the coil current, causing it to rise instead of decay during the  $T_{OFF}$  phase. Consequently, the DAC output voltage is approximately 500 mV, corresponding to a TRQ\_COUNT of 38. In contrast, when the motor is stalled, the absence of back EMF results in a uniform coil current across all quadrants, and the torque count drops to zero.

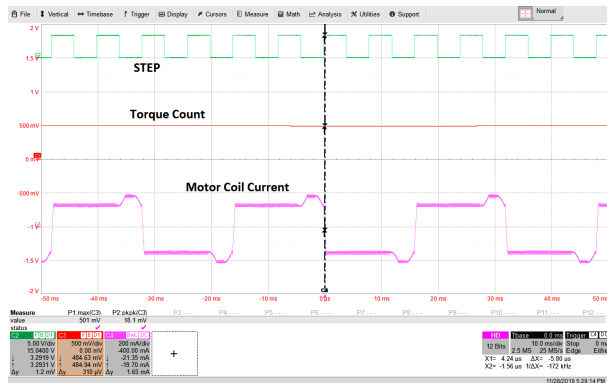


**Figure 4-4. Coil Current and Torque Count When Motor is Running**

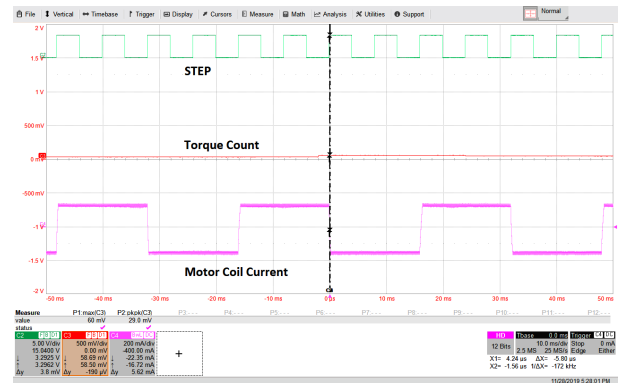


**Figure 4-5. Coil Current and Torque Count When Motor is Stalled**

#### 4.4.2 TRQ\_COUNT / STALL\_TH Resolution Analysis

This section evaluates the effect of TRQ\_COUNT and STALL\_TH resolution on sensorless stall detection by comparing the 8-bit implementation in the DRV8889-Q1 with the 12-bit implementation in the DRV8434S. The motor is operated in 1/4 microstepping mode, with a step rate of 500 PPS, a slew rate of 105 V/ $\mu$ s, and a full-scale phase current of 200 mA. The motor shaft is repeatedly driven in both inside and outside directions, followed by stall conditions in each direction to observe the corresponding TRQ\_COUNT behavior. As shown in Figure 4-6, for the DRV8889-Q1, which implements an 8-bit TRQ\_COUNT, the measured torque count during normal operation is approximately 75 counts ( $\approx$ 970 mV) representing 30% of the full 8-bit range and when the shaft moves in the outside direction and 58 counts ( $\approx$ 750 mV) during inside movement representing 22% of the full 8-bit range. Due to the 8-bit resolution, the torque counts are much coarser. In contrast, as shown in Figure 4-6, the DRV8434S provides a 12-bit TRQ\_COUNT, enabling significantly finer torque resolution. With TRQ\_SCALE disabled, the measured TRQ\_COUNT during normal movement is approximately 125 counts ( $\approx$ 100 mV), representing only about 3% of the full 12-bit range. Although the unscaled torque count occupies a smaller portion of the available range, the higher resolution allows clear differentiation between normal motion and stall. As shown in Figure 4-6, enabling the TRQ\_SCALE feature is recommended when the torque count is below 500. This scales the TRQ\_CNT and STL\_TH values by a factor of 8, thereby improving the distinction between inside movement, outside movement, and stall conditions, while reserving a fine resolution.



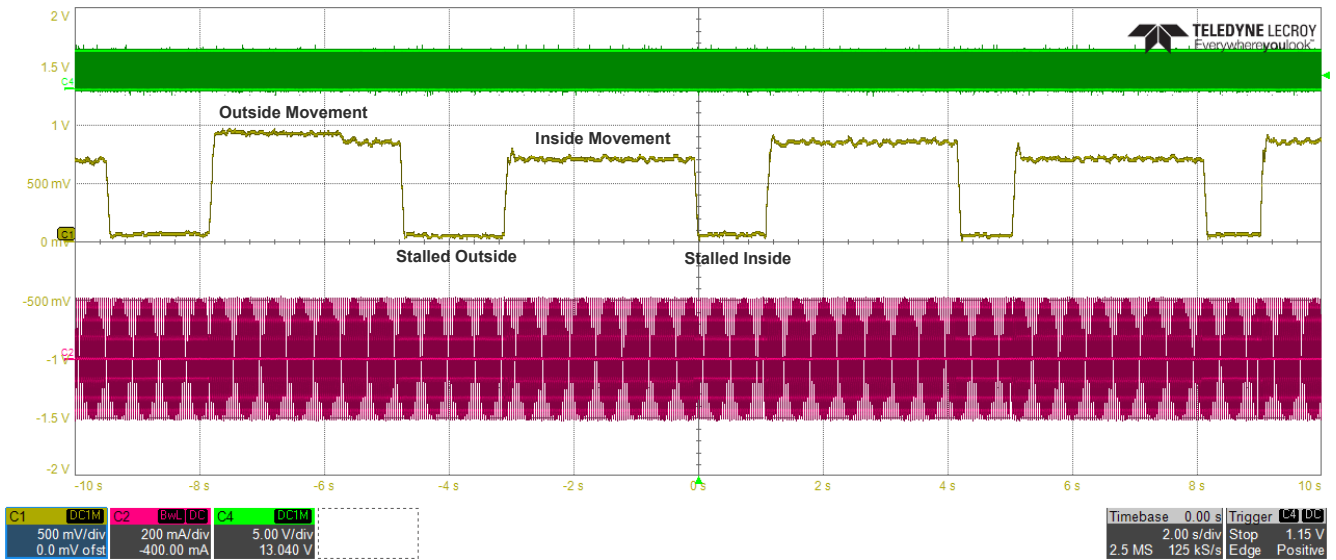


Figure 4-6. Torque Count of the PL35L-024 Motor for DRV8889

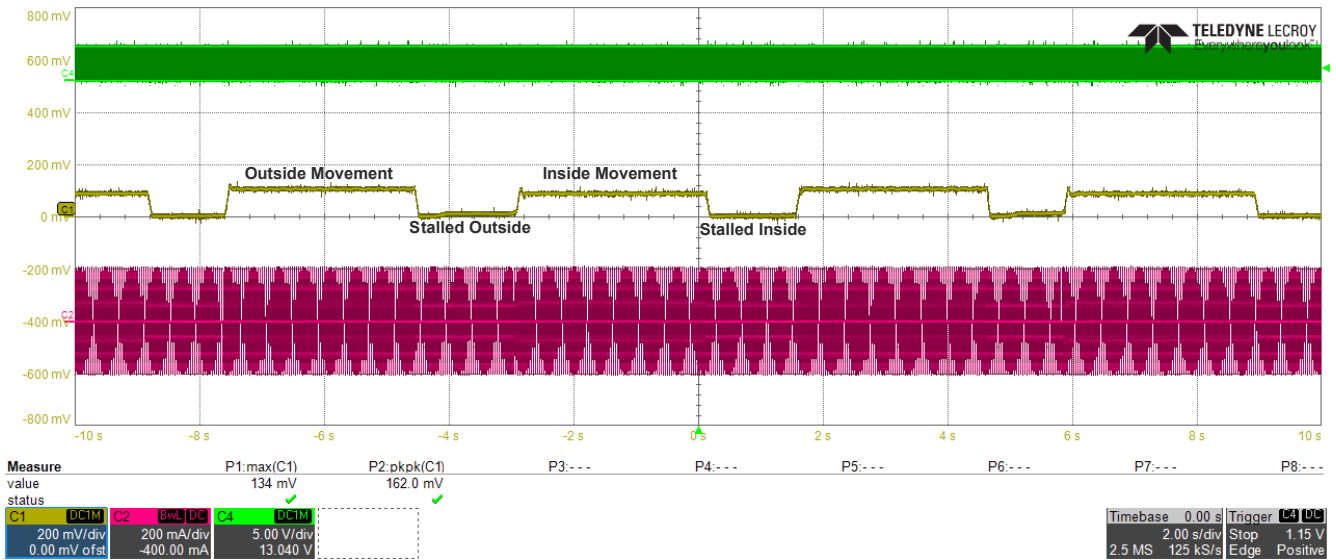


Figure 4-7. Torque Count of the PL35L-024 Motor for DRV8434S with Disabled Torque Scale

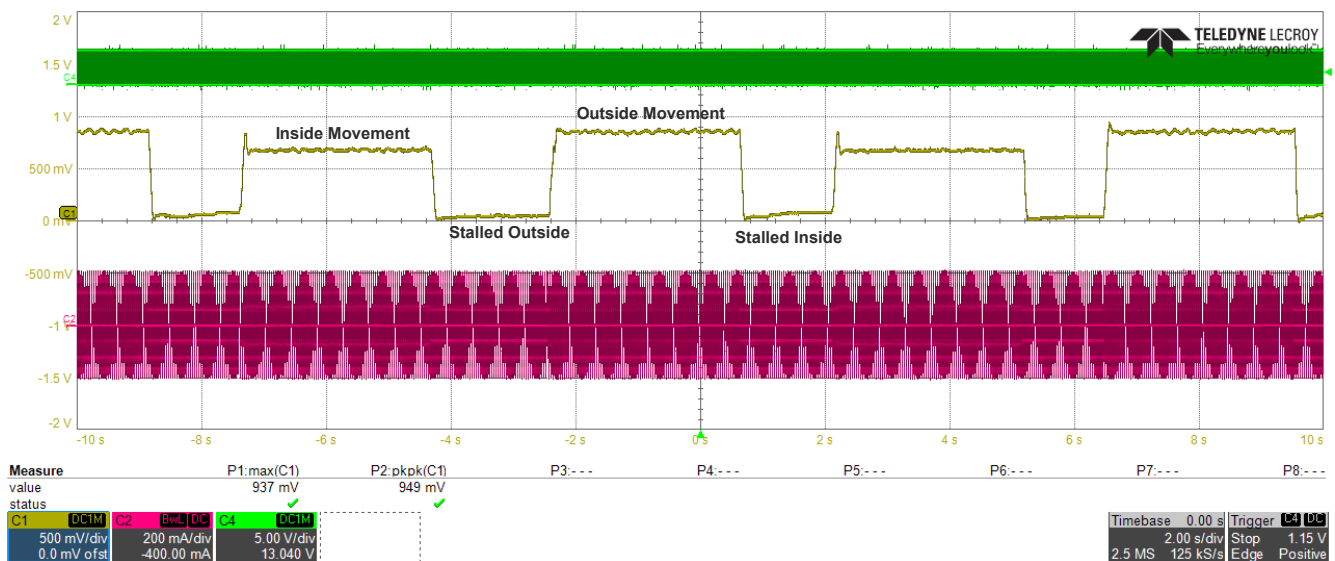


Figure 4-8. Torque Count of the PL35L-024 Motor for DRV8434S with Enabled Torque Scale

#### 4.4.3 Torque Count Variation with Operating Conditions

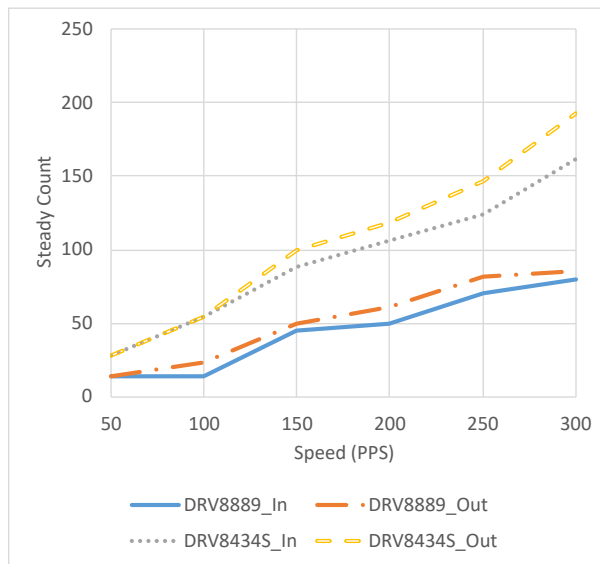
Torque count is fairly constant across variations of supply voltage, temperature, and other operating conditions. However, second-order effects will cause small variations in the torque count value, as detailed in this section.

##### 4.4.3.1 Variation With Motor Speed and Direction of Motion

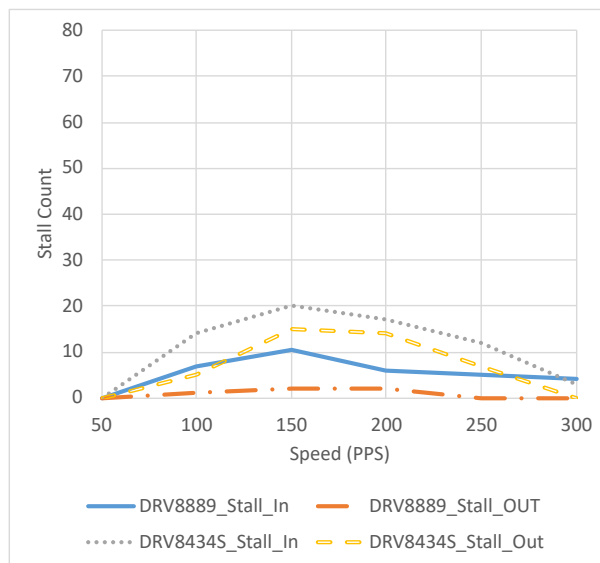
Torque count may vary with the direction of motion of the motor. The effective loading of the motor sometimes depends on the direction of the movement. For example, the rotor movement might be assisted by gravity or coil spring in one direction and opposed in the other direction. Differences in loading cause different phase changes of back EMF with respect to the coil current. This results in different steady counts, depending on the direction of motion.

Figure 4-9 shows how the steady count of the PL35L-024 motor changes depending on whether the rotor shaft is moving inside or outside. The motor was operating in full step mode, the full-scale current was set at 200 mA and the slew rate was 105 V/μs. The supply voltage was 13.5 V. Note that the steady count almost linearly increases with motor speed. This is because, the back EMF is directly proportional to motor speed. More back EMF at higher speed results in larger differences to the  $T_{OFFs}$  between rising and falling current quadrants - in other words, a larger torque count. The DRV8434S shows higher torque count due to having higher resolution.

The torque count when the motor is stalled (stall count) may also vary with the direction of motion. Stall count depends on the hardness of the end-stop. The end of travel may not actually stall the rotor - in some cases, the rotor may continue spinning due to a loose, spongy, or soft end-stop which allows the rotor to bounce. Typically, a stalled rotor vibrates as it tries to move; however, any rotational movement translates to back-EMF. Motors with large step angles may display more vibration than motors with smaller step angles. In such cases, stall count will be significantly lower than steady count, but it may not be zero. Figure 4-9 shows the stall count of the PL35L-024 motor for the same operating conditions.



**Figure 4-9. Steady Count Variation with Speed for Different Directions of Motion**



**Figure 4-10. Stall Count Variation With Direction of Motion**

#### 4.4.3.2 Limitations Due to Low Motor Speed

Low-speed operation represents the most challenging condition for stall detection due to the inherently low back-EMF value. Figure 4-11 to Figure 4-11 present steady-state torque count measurements at 150 PPS and 100 PPS using 1/8 Microstepping, comparing the DRV8889-Q1 and the DRV8434S with the TRQ\_SCALE feature enabled and disabled.

For the DRV8889-Q1, Figure 4-11 shows that at 150 PPS the torque count remains extremely low, typically below a value of 10. In addition, the relatively coarse torque count resolution results in small torque excursions that remain close to the noise floor, leading to poor separation between normal motion and stall conditions. As a result, reliable stall detection becomes increasingly difficult for the DRV8889-Q1 at low speeds.

In contrast, the DRV8434S demonstrates improved low-speed torque visibility even with TRQ\_SCALE disabled, primarily due to its higher effective torque count resolution. As shown in Figure 4-11, the torque count waveform at 150 PPS is smoother and exhibits improved granularity compared to the DRV8889-Q1. However, at very low speeds, the absolute torque count swing is still constrained by the available dynamic range, which highlights the need for torque scaling. When TRQ\_SCALE is enabled on the DRV8434S (Figure 4-11), a clear improvement is observed. Torque scaling increases the effective torque count amplitude, resulting in significantly greater

separation between normal movement and stall events. The higher resolution further enables finer discrimination between these operating states.

At 100 PPS, the limitations of the DRV8889-Q1 become more pronounced. As shown in Figure 4-11, the torque count collapses toward zero under both movement and stall conditions due to the coarse resolution, effectively preventing reliable stall detection at this speed. In comparison, the DRV8434S maintains improved torque observability even with TRQ\_SCALE disabled, as illustrated in Figure 4-11. When TRQ\_SCALE is enabled, the DRV8434S continues to clearly distinguish between movement and stall conditions even at 100 PPS, demonstrating robust torque count visibility under ultra-low-speed operation.

Overall, these results demonstrate that higher torque count resolution combined with torque scaling provides a fundamental advantage for low-speed operation. Compared to the DRV8889-Q1, the DRV8434S delivers superior torque count visibility, increased stall detection margin, and enhanced robustness at both 150 PPS and 100 PPS with 1/8 Microstepping. The addition of the TRQ\_SCALE feature further extends these benefits by maximizing the usable torque measurement range, making the DRV8434S well-suited for ultra-low-speed and high-precision motion control applications where reliable stall detection is critical.

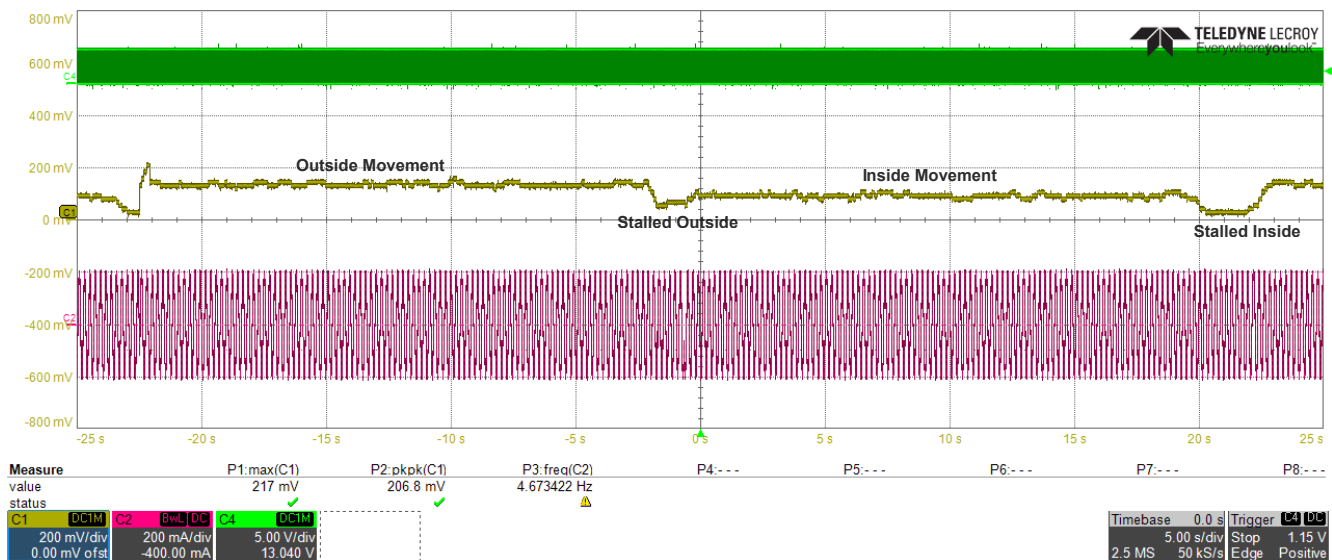


Figure 4-11. Steady Count at 150 pps for DRV8889-Q1

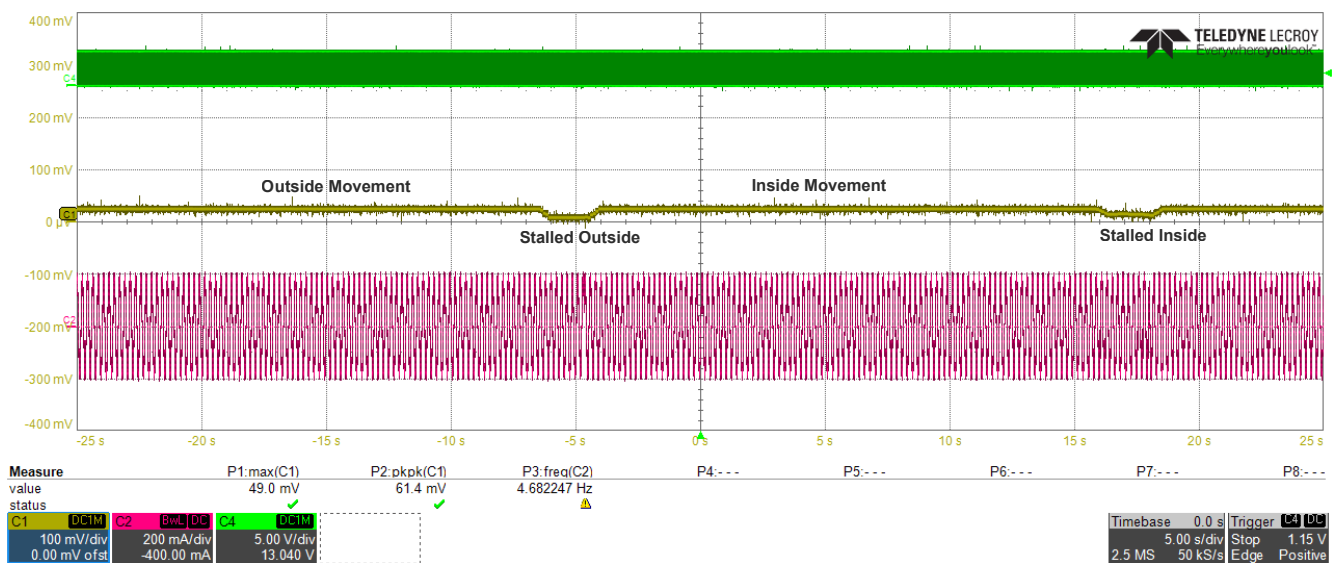


Figure 4-12. Steady Count at 150 pps for DRV8434S with Disabled TRQ\_SCALE

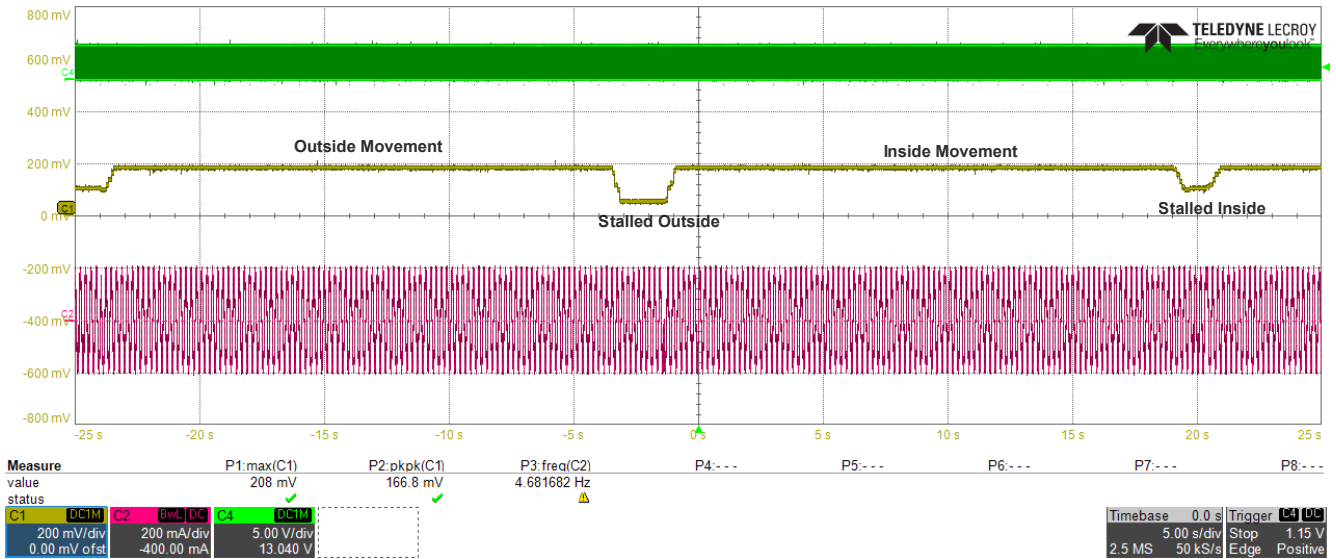


Figure 4-13. Steady Count at 150 PPS for DRV8434S with Enabled TRQ\_SCALE

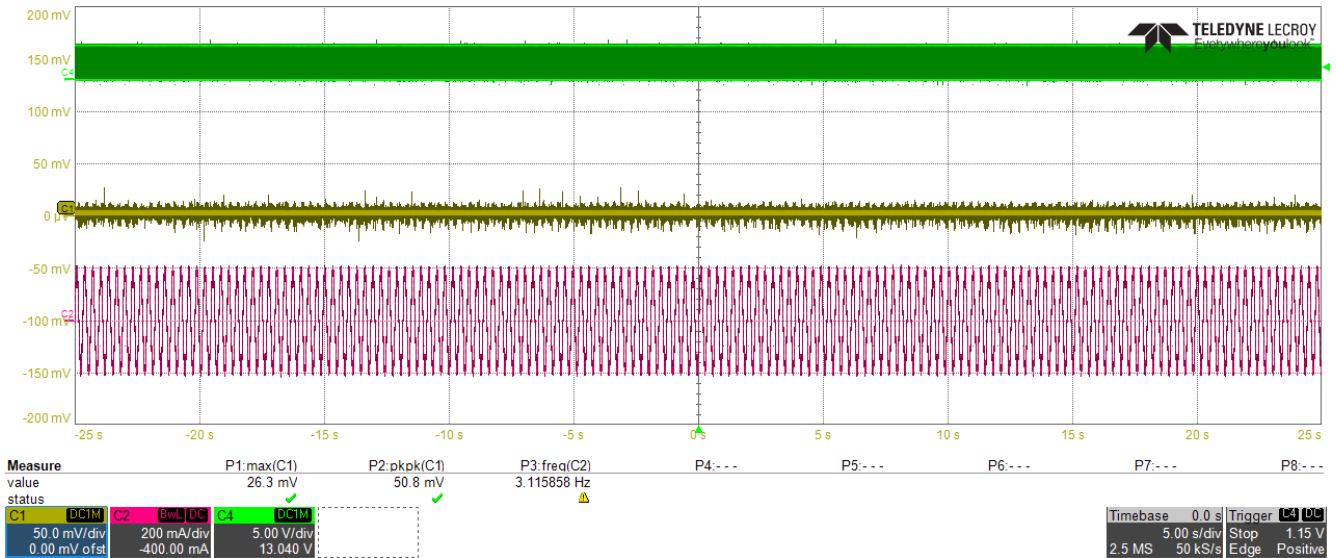


Figure 4-14. Steady Count at 100 PPS for DRV8889-Q1

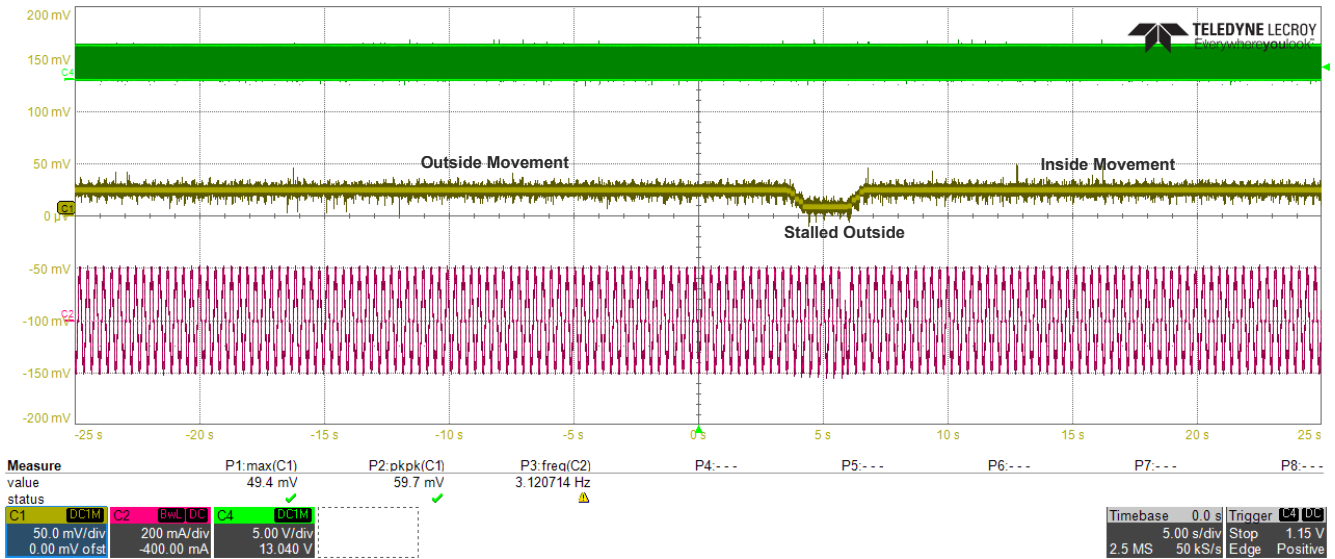


Figure 4-15. Steady Count at 100 PPS for DRV8434S with Disabled TRQ\_SCALE

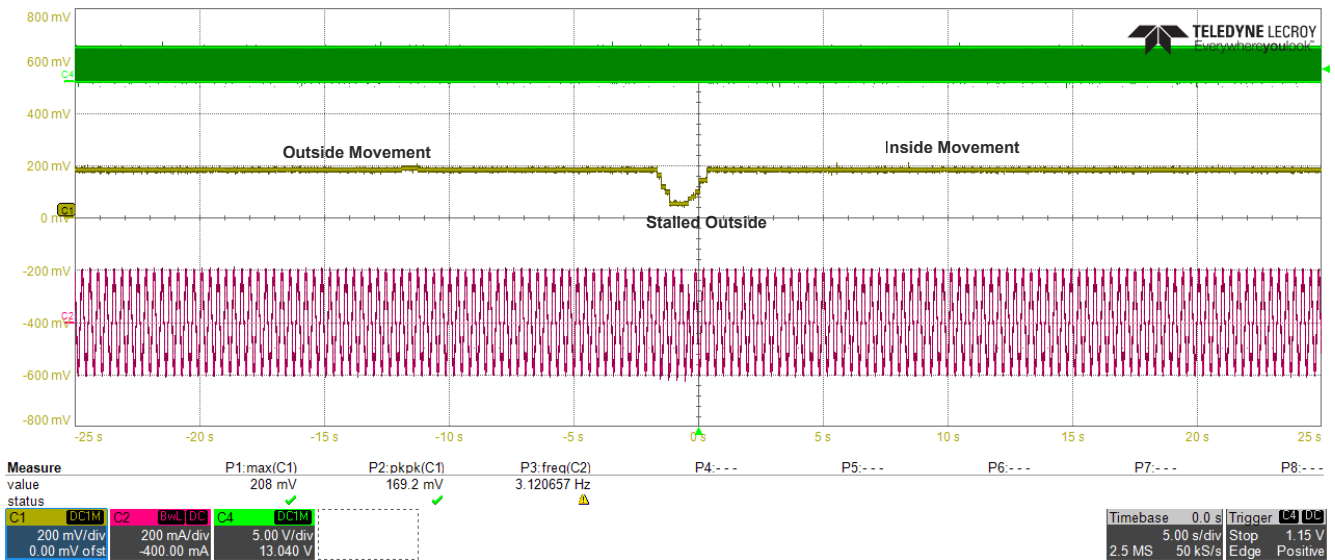


Figure 4-16. Steady Count at 100 PPS for DRV8434S with Enabled TRQ\_SCALE

#### 4.4.3.3 Limitations Due to High Motor Speed

High speed, and large back-EMF distorts the coil current and stall detection might be unreliable at very high motor speeds. The following four scope shots show the coil current in full step mode for a 17PM- F438B motor, running with 13.5-V supply voltage and 500-mA full-scale current.



Figure 4-17. Steady Count at 200 PPS

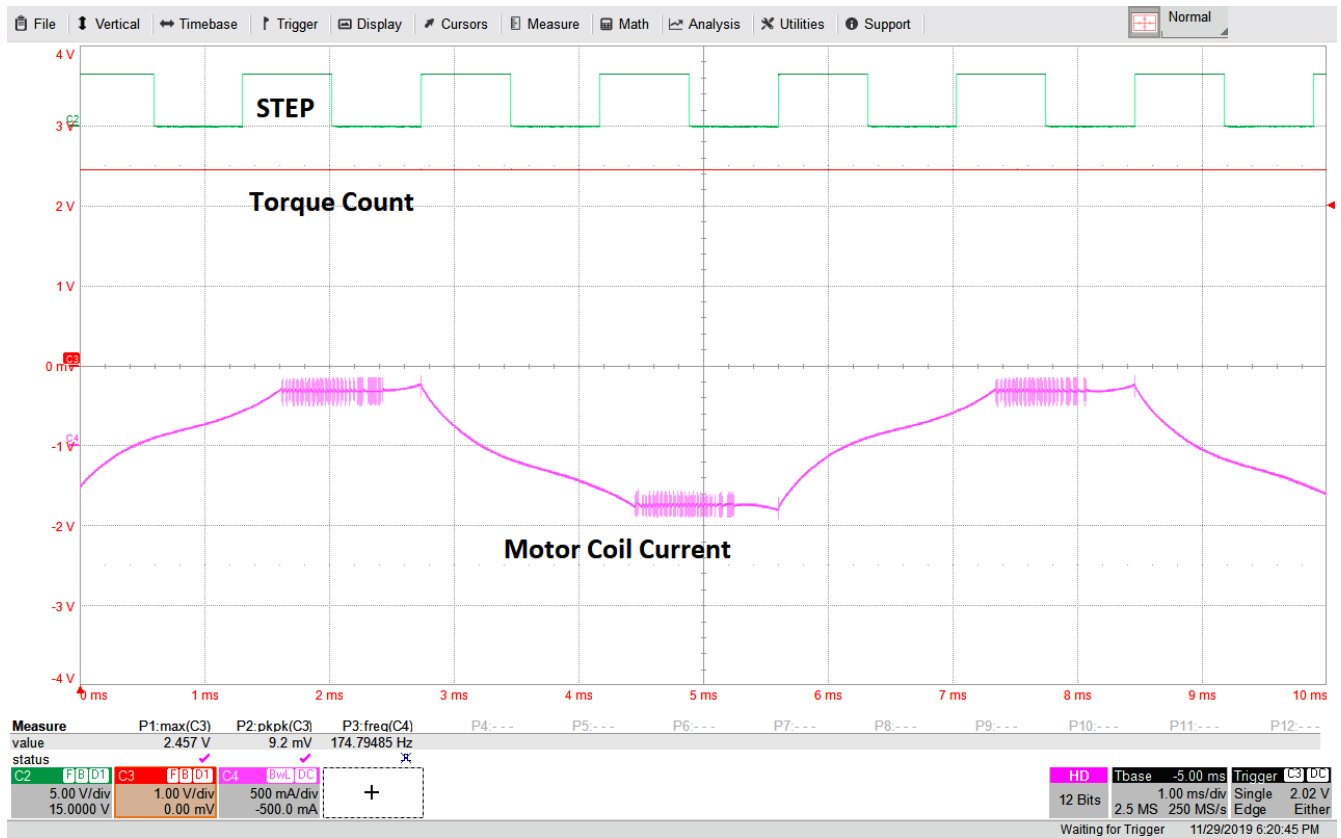


Figure 4-18. Steady Count at 700 PPS





Figure 4-19. Steady Count Change When Q1 Regulation is Lost



Figure 4-20. Steady Count at 1100 PPS

As Figure 4-17 shows, when the motor speed is such that current is regulated in both Q1 and Q2 quadrants, the algorithm uses the  $T_{OFF}$  from both quadrants and derives the torque count.

Figure 4-17 shows that at higher speeds, the rise time of the current can be so high that current regulation in Q1 will be lost, but current will still be regulated in Q2. Even in this case, stall can still be detected reliably. When current regulation is lost in Q1, it causes a sudden jump in the torque count value, as Figure 4-17 shows.

At even higher speeds ( Figure 4-17), the current waveform might be so highly distorted that regulation will be lost in both Q1 and Q2 quadrants. In such cases, the algorithm can no longer detect stall and the torque count value will be unstable and unreliable.

The rise time of the current, shown in Figure 4-17, depends on the supply voltage, coil inductance, and coil current level according to the well-known  $V = L \times di/dt$  equation. Lower rise time allows the current to be regulated at even higher speeds. Therefore, wider operating speed range can be obtained through, (1) a motor with low inductance, (2) lower current level, and (3) higher supply voltage.

#### 4.4.3.4 Variation With Supply Voltage

Equation Equation 5 states that the  $T_{OFF}$  parameter is independent of supply voltage (VM). Therefore, when the average of  $T_{OFF}$  from one quadrant is compared to the average of  $T_{OFF}$  from the next quadrant, the result should be independent of supply voltage. However, Figure 4-21 shows that there is small variation in the steady count with supply voltage. This data is for the PL35L-024 motor, at 1/8 microstepping with 1000 PPS speed, 105 V/ $\mu$ s slew rate, and full-scale current set at 200 mA.

This variation can be explained by looking at the current ripple at various supply voltages. At higher voltages, the ripple increases slightly, which results in a slight increase in the  $T_{OFF}$  value. However, the change in  $T_{OFF}$  for the Q2 quadrant will be slightly larger than the  $T_{OFF}$  change in Q1, because the back-EMF magnitude remains constant at higher voltages. The effect of this is the slight increase in steady count with supply voltage.

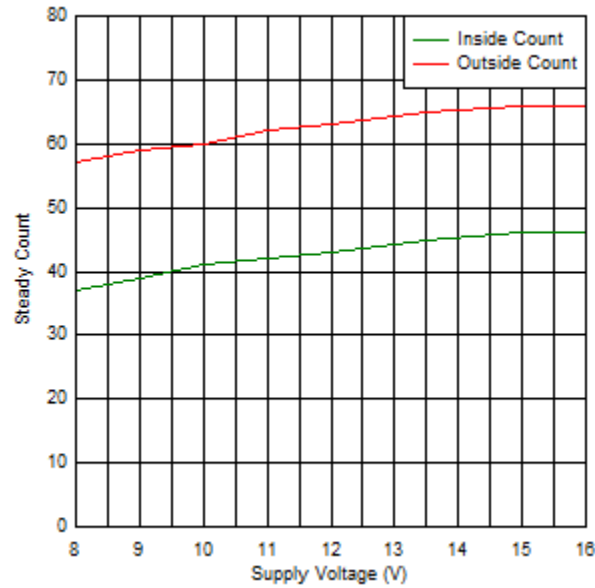


**Figure 4-21. Steady Count Variation With Supply Voltage**

#### 4.4.3.5 Variation With Microstepping Setting

Higher-order microstepping generally results in a higher torque count. Figure 4-22 shows the variation in steady count with microstepping settings for the PL35L-024 motor. The motor speed (PPS) was adjusted at each microstepping to arrive at the same 125 full steps per second rate.

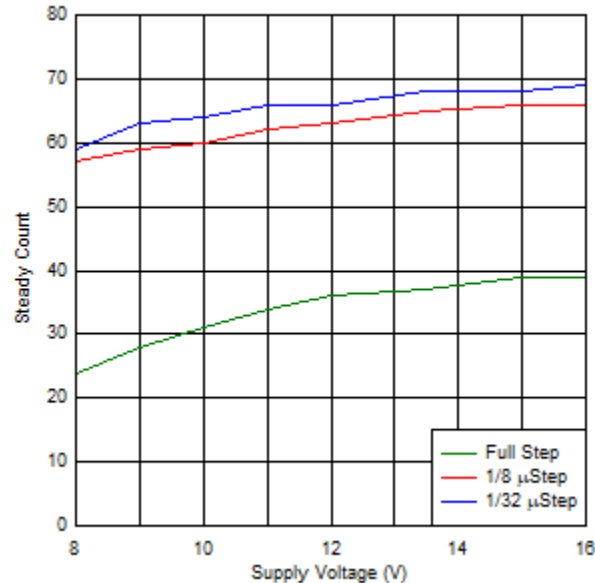


**Figure 4-22. Steady Count Variation With Microstepping**

#### 4.4.3.6 Variation With Output Slew Rate

Slower output slew rate results in a lower torque count. Due to slower output fall time, the  $T_{OFF}$  decreases at a slower slew rate, which leads to lower torque count.

Higher slew rates are also preferable to keep the switching loss of the driver to a minimum - allows the driver to support higher currents at a given ambient temperature. Conversely, lower slew rates result in better EMC performance. A careful trade-off analysis needs to be carried out to select the proper slew rate for an application.

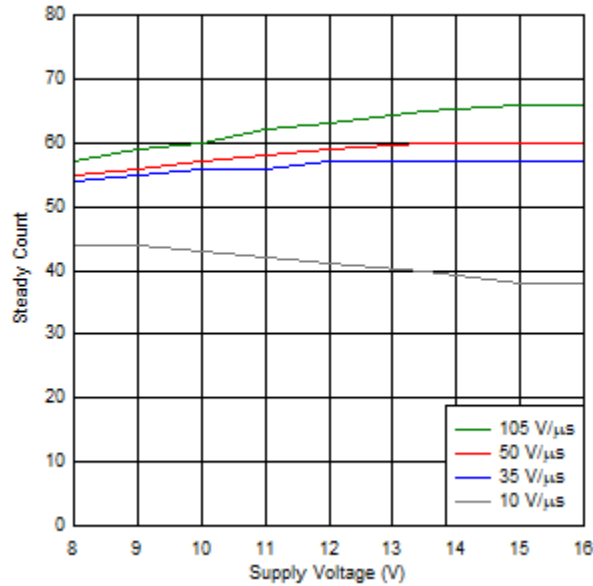


**Figure 4-23. Steady Count Variation With Output Slew Rate**

**4.4.3.7 Variation With Ambient Temperature**

Figure 4-24 shows how the inside and outside counts change with ambient temperature for a stepper used in a HVAC gas valve. The motor was running at full-step mode with 300 PPS speed. As is evident from the plot, the torque count is almost independent of the ambient temperature.

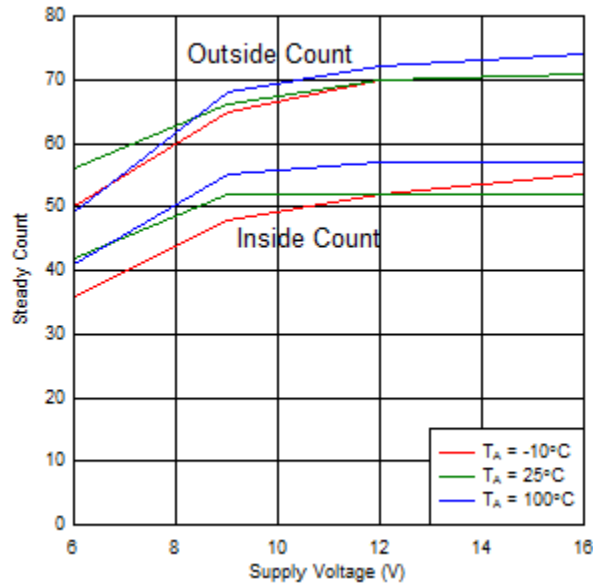


**Figure 4-24. Steady Count Variation With Ambient Temperature**

#### 4.4.3.8 Variation With Full-Scale Current Setting

At a constant supply voltage, steady count drops at higher full-scale current. High  $I \times R_{coil}$  drop across the motor coil leaves too little back EMF; therefore, the  $T_{OFF}$  does not get affected, causing lower count.

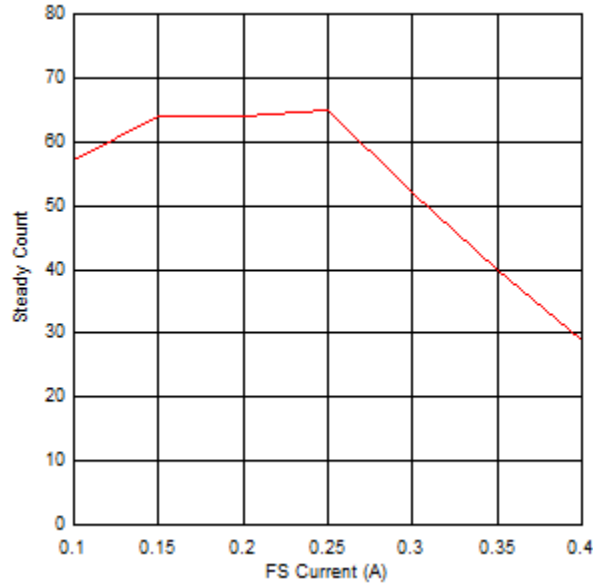


**Figure 4-25. Steady Count Variation With Full-scale Current**

##### 4.4.3.8.1 Limitations Due to High Coil Resistance

If the coil resistance is too high, the coil current waveform is distorted and the back EMF is unable to influence the  $T_{OFF}$  - resulting in unreliable torque count and stall detection.

Figure 4-26 shows the coil current waveform for an HVAC valve motor with 80-Ω resistance. The supply voltage was 12 V, and the full scale current was 200 mA. It is clear that the torque count waveform is erratic in nature and a stall cannot be reliably detected. Figure 4-26 shows the torque count for another HVAC motor with 36-Ω coil resistance at the same operating condition. When the motor is stalled at one end, there is periodic vibration - leading to spikes in the stall count. Even though there is some overlap between steady count and stall count, using an external low-pass filter with sufficiently high time-constant to eliminate the spikes in the stall count can result in reliable stall detection.

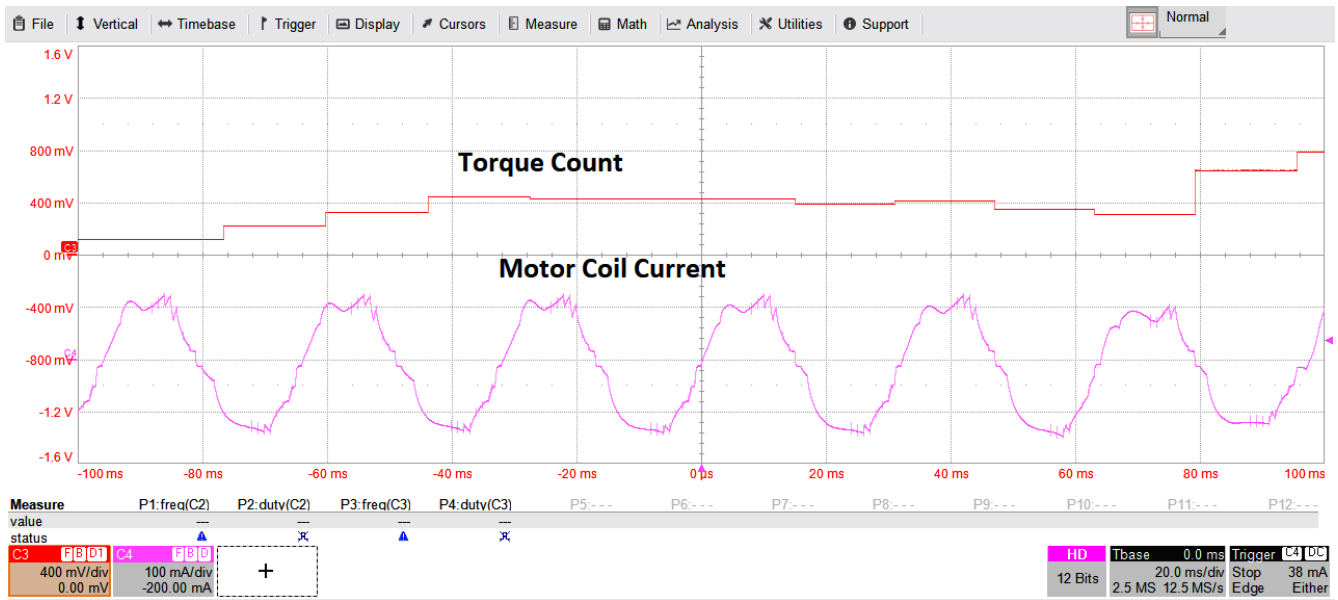


Figure 4-26. Coil Current Waveform for a Valve Motor With 80-Ω Resistance

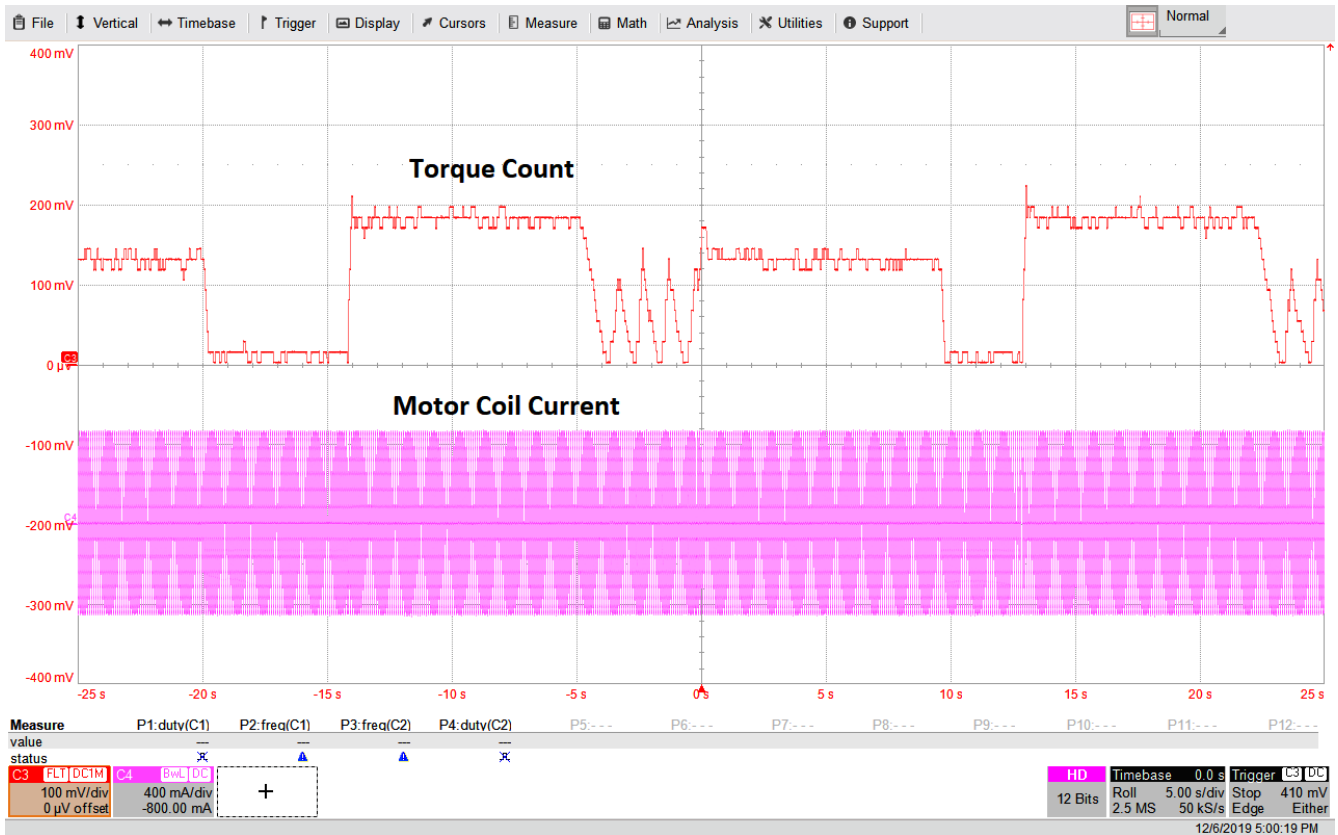


Figure 4-27. Coil Current Waveform for a Valve Motor With 36-Ω Resistance

#### 4.4.3.9 Steady-State Count Variation at a Fixed Operating Condition

Figure 4-28 shows the steady count of the PL35L-024 motor, running at 1/8 microstepping and 1000 PPS speed. The waveform has a peak-to-peak ripple of 42 mV, corresponding to a count variation by 3. In other words, steady count is varying between 63 and 66. This can be explained by small random variations in the  $T_{OFF}$  due to several factors - such as the nature of the back-EMF voltage and minor asymmetries in motor construction.

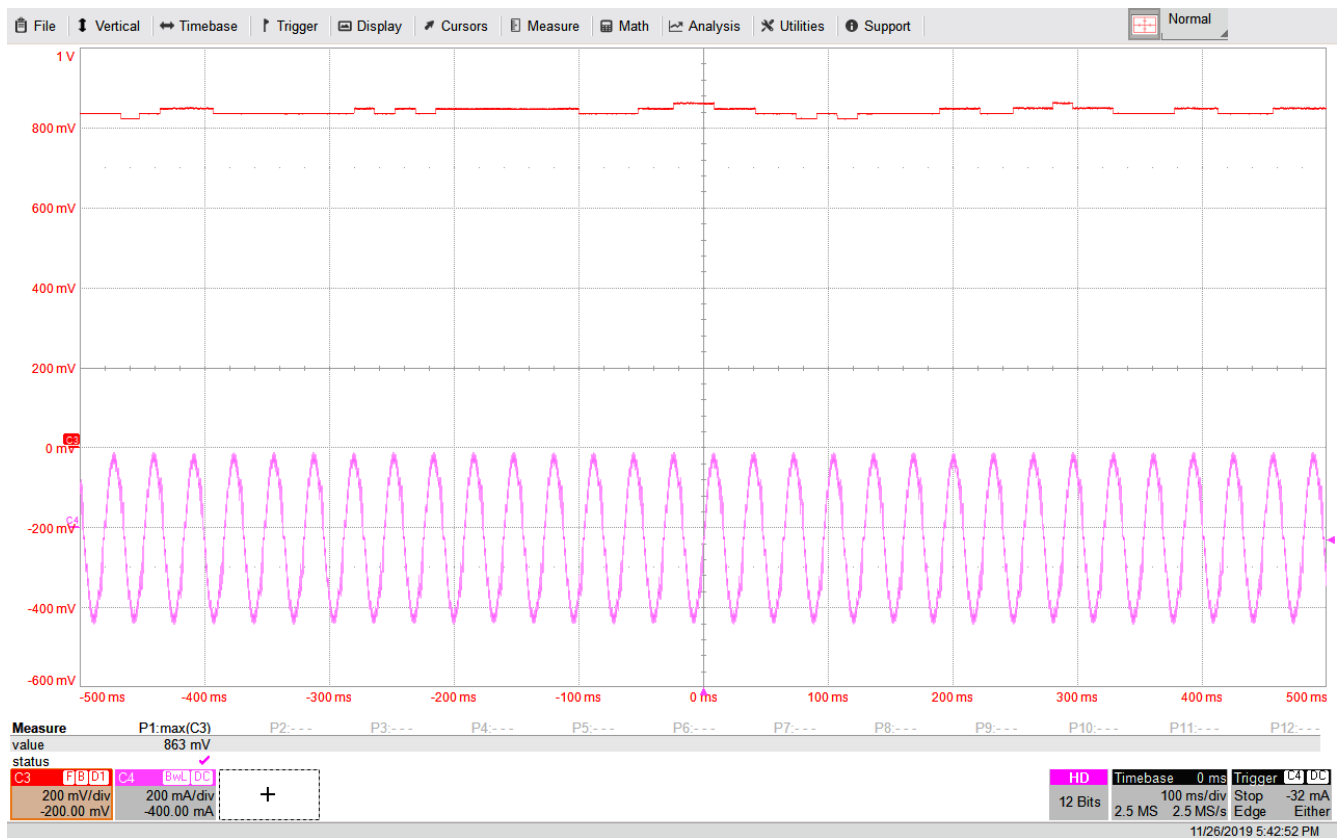


Figure 4-28. Steady-State Torque Count Variation

## 5 Evaluation Examples

### 5.1 Automotive Headlight Leveling and Swivel

Adaptive front lighting (AFS) systems are widely used by car manufacturers across geographical locations. These systems compensate for changes in the inclination of the vehicle relative to the road surface by making slight vertical adjustments to the light beam of the headlamp. They also cause the headlamps to swivel in response to a change in the turning direction of the vehicle. Stepper motors are often used for headlamp adjustment applications because stepper motors are low cost, rugged, and provide a high torque in relation to their size.

Most automotive headlamp systems require stall detection, to prevent the motor from hitting end-stop during the initial position calibration or during normal operation. Without stall detection, to ensure that the end-stop is reached, the stepper motor is driven multiple steps beyond the estimated end-stop position. This results in a blocked motor with associated audible noise and mechanical wear-out. Audible noise is particularly sensitive for electric vehicles. Without integrated stall detection, some systems are forced to use expensive position sensors to receive feedback about the angular location of the motor.

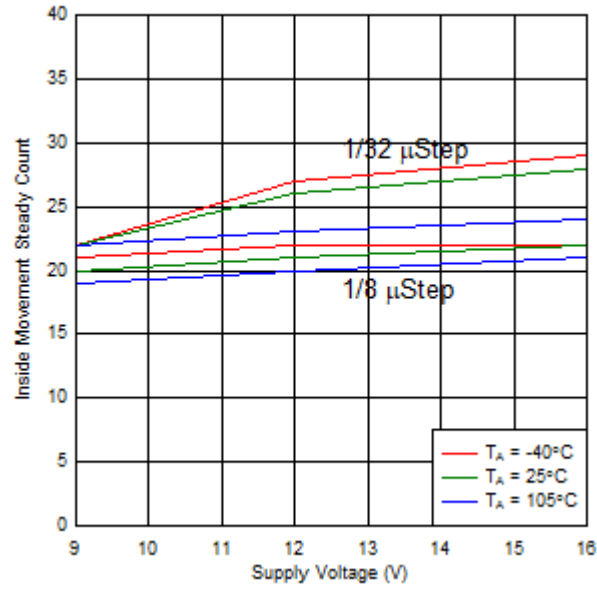
The following example shows how the DRV8889-Q1 detects stall for an automotive headlight module. While running, the rotor shaft moves inside or outside and can get stalled at both ends. The operating conditions for this typical adaptive headlight application are listed in [Table 5-1](#).

Table 5-1. Operating Conditions for Headlight Stepper Motor

Parameter	Value
Supply voltage range	9 V to 16 V
Full scale current	500 mA
Target speed	122.5 Full-steps/s
Microstepping	1/8 or 1/32

**Table 5-1. Operating Conditions for Headlight Stepper Motor (continued)**

Parameter	Value
Temperature range	-40°C to 105°C
Motor coil resistance	7.7 Ω
Motor step angle	15°



**Figure 5-1. Steady Count Across Operating Conditions**



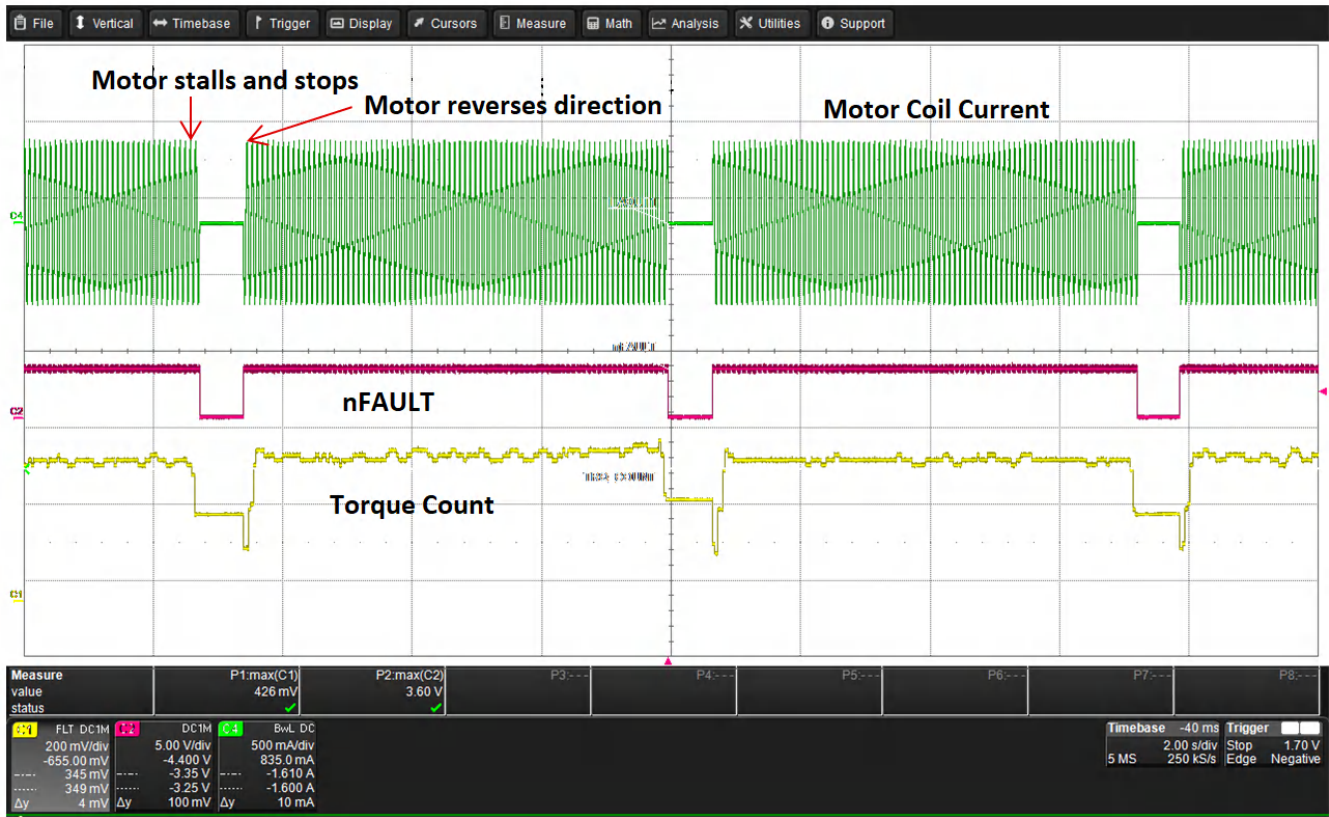


Figure 5-2. Stall Detection of a Headlight Module With DRV8889-Q1

Figure 5-1 plots the steady count for the inside movement as a function of the operational parameters of the headlight module. The inside direction count is lower than the outside direction count. Based on the minimum inside count, a stall threshold of 12 was selected. With this stall threshold, the DRV8889-Q1 detects stall reliably at both ends of operation across operating conditions, as Figure 5-2 shows. The nFAULT output goes low whenever the torque count is lower than the stall threshold, indicating to the system that stall has been detected.

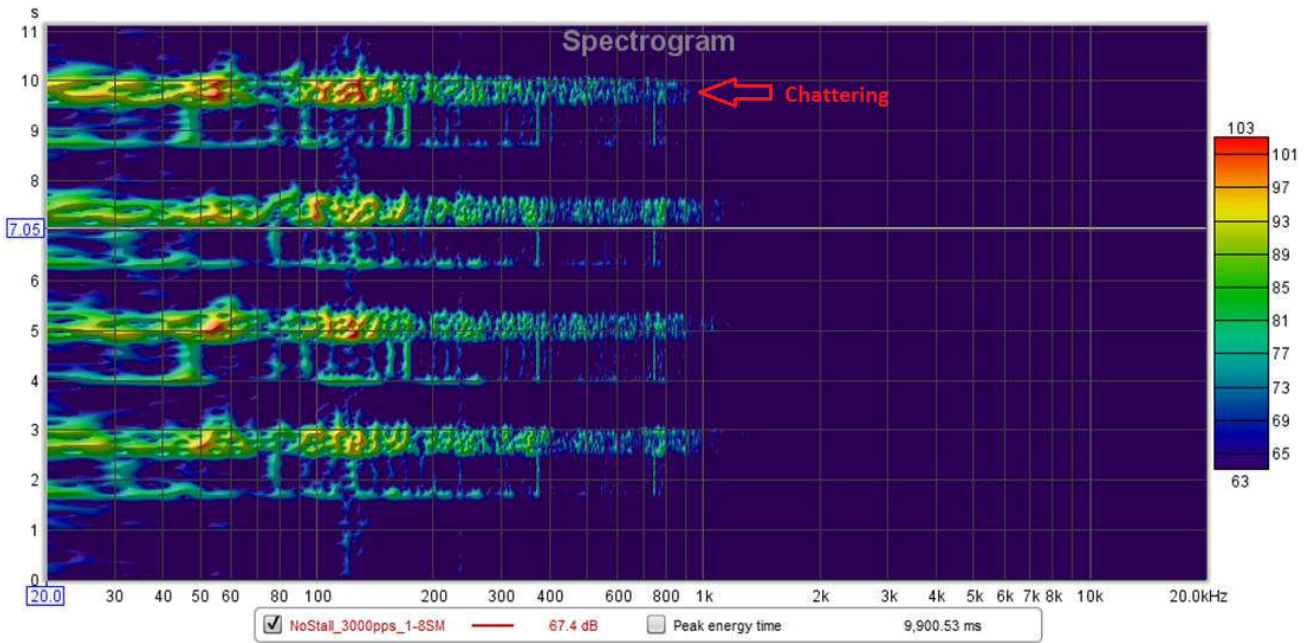


Figure 5-3. Audio Noise Spectrogram Without Stall Detection

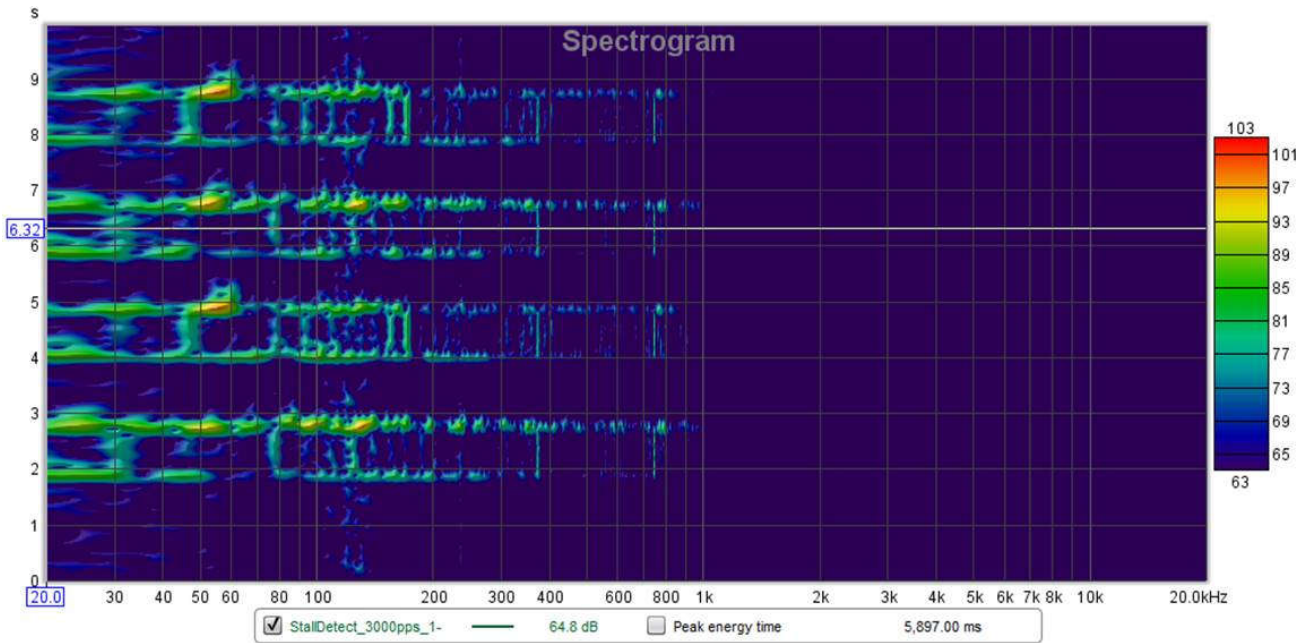


Figure 5-4. Audio Noise Spectrogram With DRV8889-Q1 Stall Detection

Figure 5-3 and Figure 5-3 show the audio noise spectrograms for two cases – one in which the headlight module operates without stall detection and the other in which the module uses the DRV8889-Q1 device to detect stall at both ends. Figure 5-3 clearly shows the evidence of large audio noise at approximately 55 Hz and between 100 Hz and 200 Hz. This spectrogram also shows how the stepper motor chatters when it reaches the end-of-line – an effect of the over-drive needed to ensure that the motor has indeed reached the end. Conversely, Figure 5-3 shows that the audio noise is largely absent – more so between 100 Hz and 200 Hz, and the chattering is also non-existent.

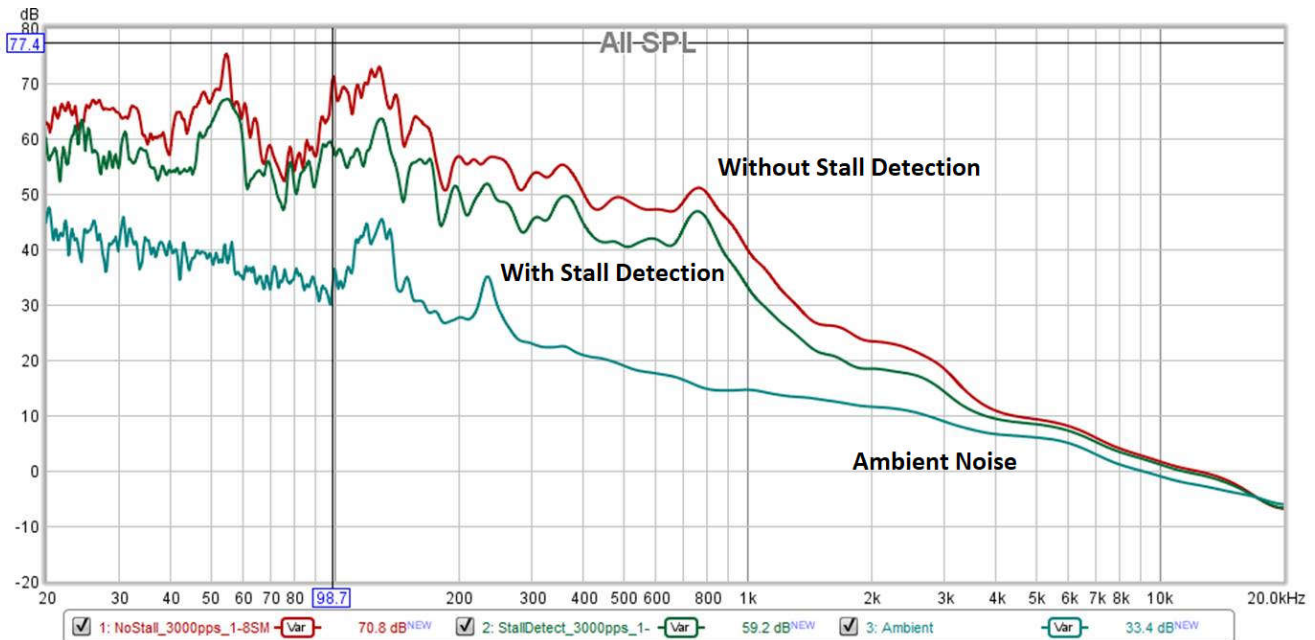


Figure 5-5. Audio Noise SPL Plot With and Without Stall Detection

Figure 5-3 shows the reduction in audible noise with stall detection. Clearly, with stall detection, there is more than 10-dB improvement in the noise level at some frequencies.

## 5.2 Automotive Head-up Display (HUD)

Automotive Head-Up Displays (HUD) are intended to assist drivers by projecting important trip information such as speed, navigation data, RPM, alerts, and augmented reality overlays onto the inside surface of the windshield or a transparent piece of plastic called a 'combiner'. The system requires multiple lenses and mirrors to project the information onto the windshield or combiner, and the mirrors must be rotated with precision to achieve accurate positioning. Therefore, a lot of HUD units use stepper motors, and sensorless stall detection is often a requirement to ensure that the mirrors reach their end stop without resulting in excessive audio noise or mechanical wear-out.

The following example shows how the DRV8889-Q1 device detects stall for an automotive HUD module. This combiner HUD module uses a custom bipolar stepper motor, which moves a reflector mirror up and down. The operating conditions of the HUD application and details of the stepper motor are shown in [Table 5-2](#).

**Table 5-2. Operating Conditions for HUD Module**

Parameter	Value
Operating voltage range	8 V to 16 V
Full-scale current	180 mA
Target speed	2550 PPS
Microstepping	1/32
Temperature range	-40°C to +85°C
Motor coil resistance	20 Ω ±7%
Step angle	0.514° / STEP

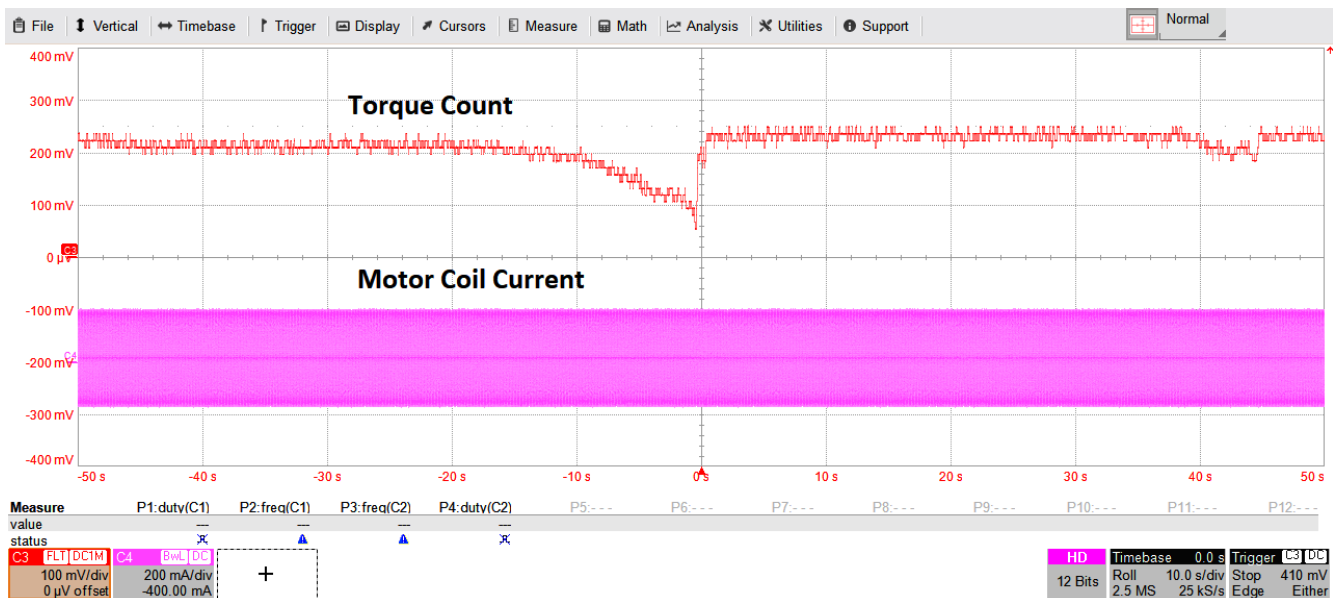


**Figure 5-6. Stall Detection**

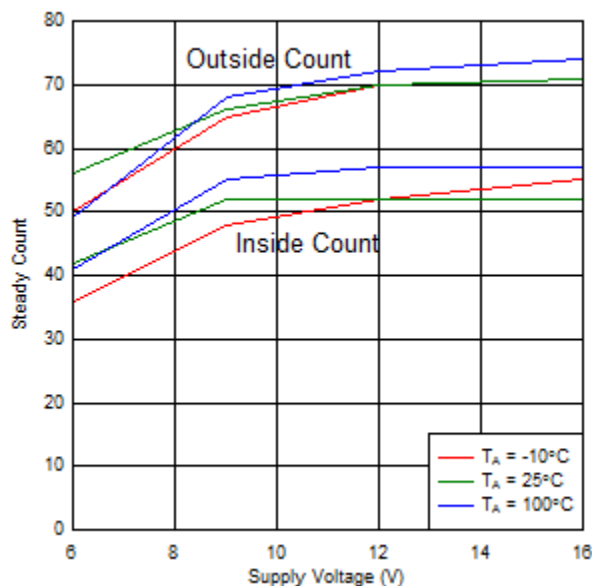
show how the torque count decreases during motor stall. A stall threshold of 120 mV (corresponding to TRQ\_COUNT = 10) will detect stall reliably across corners for this application.

## 5.3 HVAC Valve Control

HVAC valve control actuators also require stall detection. A stepper motor driver with integrated sensorless stall algorithm allows precise detection of the end-stop of a flap or a valve tip in an HVAC system, without requiring over-drive of the stepper motor. The following example shows how the DRV8889-Q1 detects stall for an HVAC valve. The operating conditions of this HVAC application are shown in [Table 5-2](#).

**Table 5-3. Operating Conditions for HVAC Valve**

Parameter	Value
Operating Voltage Range	6 V to 16 V
Full Scale Current	300 mA
Target Speed	300 steps/sec
Microstepping	Full-step
Temperature range	-30 °C to +100 °C

**Figure 5-7. HVAC Valve Steady Count**

The valve motor gets stalled at both ends of the movement. [Figure 5-7](#) shows the steady count in both directions as a function of the supply voltage. A stall threshold of 30 works well to reliably detect stall at both the ends of the valve tip movement.

## 6 Summary

Various sensorless stall detection schemes are available from different manufacturers. The novel stall detection scheme implemented in the stepper drivers from Texas Instruments can reliably detect stall for various applications over a wide range of supply voltage, speed, and other operational parameters. The robustness of the algorithm, combined with the ease of use, makes these stepper drivers an ideal option to replace costly position sensors used to send positional feedback in a wide range of end applications.

## 7 References

- Acarnley, Paul P. *Stepping motors: a guide to theory and practice*. 4th ed., Institution of Engineering and Technology, 2007.
- [Methods and apparatus for robust and efficient stepper motor BEMF measurement](#), by Sooping Saw, Rakesh Raja, Anuj Jain and Matthew Hein; *United States Patent US10063170B2*
- [Stall detection in stepper motors using differential back-emf between rising and falling commutation phase of motor current](#), by Sooping Saw, Rakesh Raja, Wen Pin Lin and Sudhir Nagaraj; *United States Patent US20190109551A1*
- Texas Instruments, [DRV8889-Q1 Automotive Stepper Driver with Integrated Current Sense, 1/256 Microstepping, and Stall Detection](#), data sheet
- Texas Instruments, [DRV8434A Stepper Driver With Integrated Current Sense, 1/256 Microstepping, smart tune and Stall Detection using GPIO pins](#), data sheet
- Texas Instruments, [DRV8434S Stepper Driver With Integrated Current Sense, 1/256 Microstepping, SPI Interface, Smart Tune Technology and Stall Detection](#), data sheet

- Texas Instruments, [DRV8461: 65 V, 3 A Stepper Motor Driver for High Efficiency and Noiseless Operation](#), data sheet
- Texas Instruments, [DRV8452: 55 V, 5 A Stepper Motor Driver for High Efficiency and Noiseless Operation](#), data sheet
- Texas Instruments, [DRV8462: 65 V, 5-10 A Stepper Motor Driver for High Efficiency and Noiseless Operation](#), data sheet

## 8 Revision History

<b>Changes from Revision * (September 2020) to Revision A (February 2026)</b>	<b>Page</b>
• Updated the TI devices with stall detection feature.....	<a href="#">1</a>

---

## IMPORTANT NOTICE AND DISCLAIMER

TI PROVIDES TECHNICAL AND RELIABILITY DATA (INCLUDING DATASHEETS), DESIGN RESOURCES (INCLUDING REFERENCE DESIGNS), APPLICATION OR OTHER DESIGN ADVICE, WEB TOOLS, SAFETY INFORMATION, AND OTHER RESOURCES "AS IS" AND WITH ALL FAULTS, AND DISCLAIMS ALL WARRANTIES, EXPRESS AND IMPLIED, INCLUDING WITHOUT LIMITATION ANY IMPLIED WARRANTIES OF MERCHANTABILITY, FITNESS FOR A PARTICULAR PURPOSE OR NON-INFRINGEMENT OF THIRD PARTY INTELLECTUAL PROPERTY RIGHTS.

These resources are intended for skilled developers designing with TI products. You are solely responsible for (1) selecting the appropriate TI products for your application, (2) designing, validating and testing your application, and (3) ensuring your application meets applicable standards, and any other safety, security, regulatory or other requirements.

These resources are subject to change without notice. TI grants you permission to use these resources only for development of an application that uses the TI products described in the resource. Other reproduction and display of these resources is prohibited. No license is granted to any other TI intellectual property right or to any third party intellectual property right. TI disclaims responsibility for, and you fully indemnify TI and its representatives against any claims, damages, costs, losses, and liabilities arising out of your use of these resources.

TI's products are provided subject to [TI's Terms of Sale](#), [TI's General Quality Guidelines](#), or other applicable terms available either on [ti.com](http://ti.com) or provided in conjunction with such TI products. TI's provision of these resources does not expand or otherwise alter TI's applicable warranties or warranty disclaimers for TI products. Unless TI explicitly designates a product as custom or customer-specified, TI products are standard, catalog, general purpose devices.

TI objects to and rejects any additional or different terms you may propose.

Copyright © 2026, Texas Instruments Incorporated

Last updated 10/2025